A state of the art of required techniques for employing activated carbon in renewable energy powered adsorption applications

Ahmed M. Elsayed[a,b], Ahmed A. Askalany[c], Andrew D. Shea[a], Hassan J. Dakkama[d,e], Saad Mahmoud[d], Raya Al-Dadah[d,] Waseem Kaialy[f]

[a]BRE Centre for Innovative Construction Materials, Department of Architecture & Civil Engineering, University of Bath, Bath, BA2 7AY, UK

[b]Alexandria university, Department of Mechanical engineering, Egypt

[c]Mechanical Engineering Department, Faculty of Industrial Education, Sohag University, Sohag, 82524, Egypt

[d]School of Mechanical Engineering, University of Birmingham, UK

[e]Middle Technical University, Faculty of Engineering, Baghdad, Iraq

[f] School of Pharmacy, Faculty of Science and Engineering, University of Wolverhampton, WV1 1LY, UK

Abstract

This paper reviews, for the first time, the measurement adsorption characteristics techniques to facilitate optimal testing of the validity of adsorbent materials in adsorption applications. Thermo-physical properties, adsorption characteristics and modelling techniques are presented. The characterisation of material thermo-physical properties includes true and bulk densities, specific heat capacity, surface area, pore volume distribution and thermal conductivity. The adsorption characteristics were categorized into adsorption isotherms and kinetics including experimental and theoretical equations. A range of models used in the simulation of adsorption cooling

systems is presented and discussed. The paper highlights the conditions for which each measurement technique is most suitable and the limitations of modelling techniques, which is a vital element in the robust assessment of the performance of adsorption cooling units.

Keywords: Activated carbon; Adsorption cooling; Adsorption kinetics; Isotherms.

1. Introduction

Worldwide, building air-conditioning systems consume more than 15% of all generated electricity. Such significant electrical energy consumption leads to depletion of fossil fuel resources and production of greenhouse gases. Heat-driven cooling systems utilize waste and/or renewable energy such as automobile exhausts and solar thermal energy to produce a cooling effect with correspondingly lower environmental impact. One such system is sorption cooling which has low global warming potential (GWP) and zero ozone depletion potential (ODP). In recent decades, absorption (liquid/vapour) cooling systems have become commercially available technology, but they still suffer from corrosion, toxicity and crystallisation of the working fluids. Adsorption cooling (solid / vapour) offers several advantages including relatively low electricity consumption (no circulating pump), low driving heat source temperature and high operational reliability due to the low number of moving parts [1-4].

Common adsorbents, which have been studied extensively and employed in adsorption cooling applications, include zeolite, silica gel and activated carbon [5-7]. The activated carbon materials have been used with various refrigerants to produce adsorption cooling systems for low-temperature applications [8-11]. Activated carbon pairs are proposed in this investigation because they have a large surface area and relatively low cost. These adsorbents are manufactured from natural materials and indicate promising performance through chemical modification of their surface characteristics. However, while the advantages of adsorption cooling systems are clear, there remains a number of sub-optimal characteristics such as low performance and relatively high specific volume. Accordingly, much recent research has been targeted towards improving the performance of adsorption cooling systems, including the identification of new adsorption pairs, the improvement of heat transfer coefficient of adsorbents, and the presentation of new applications for adsorption techniques [12-16]. There are accepted stages in the investigation of new adsorbents to determine sufficient data for the validation of performance and suitability in adsorption cooling applications. These steps include i) measuring their physical properties such as density, thermal conductivity and specific heat, ii) establishing their adsorption isotherms, iii) determining their adsorption kinetics, iv) simulating their duty in a modelled adsorption cooling system, and v) evaluating their application in an experimental adsorption cooling system.

Although the above five steps can be considered a suitably robust testing protocol for any new adsorbent, there is no agreed method for evaluating each of the five stages and therefore numerous different methods have been employed. The aim of the current review was therefore to present these different techniques for determining material thermo-physical properties, adsorption isotherms, adsorption kinetics, and computational modelling techniques with a specific focus on the use of activated carbon.

2. Activated Carbon

Activated carbon is a solid material used in granular or powder form, it is black in colour and has the general appearance of charcoal. It is prepared in two stages by, firstly, the carbonization of carbonaceous raw material which is treated in an inert atmosphere at temperatures below 800 °C, and secondly, the activation of the carbonized product **[8]** as shown in Fig. 1. In the first stage, the cross-linkages between carbon atoms are broken down in the absence of oxygen. At this stage, the adsorbent still has poor adsorbing characteristics as the pores are blocked by carbonization by-products [11]. However, during the activation process, an enhancement of the porosity is triggered by cleaning out of the pores, which occurs through three stages, namely carbonized surface cleaning and exposure to the activating agent, then burning of elementary crystals, and lastly, oxidation with a reduction in the total micro pore volume.

There is a wide range of activated carbon materials reported in the literature, which could be classified according to their (i) physical form, e.g. powders, pellets, or granules; (ii) original carbonaceous source, e.g. olive stones **[10]**, oil palm biomass **[11]**, guava seed-based, and coconut-shell; and (iii) carbon activation methods, e.g. activation by gases or chemicals **[6]**. Activated carbon has a non-polar or slightly polar structure, which facilitates adsorbing non-polar and slightly polar organic molecules (e.g. ammonia, ethanol and methanol) to a level that is higher than other sorbents. Also, the heat of adsorption, or bond strength, is generally lower in the case of activated carbon compared to other sorbents **[6]**. Fig. 2 presents the adsorption characteristics of activated carbon materials with ethanol, carbon dioxide, HFC134a and methanol with adsorbent Maxsorb III that has a surface area of 3045 m^2/g (manufactured by Kansai Coke and Chemicals Co. Ltd) . Due to the slow kinetics of Maxsorb III–ethanol pair, it is a candidate adsorbent for solar adsorption cooling where cycle time effect has low importance.

3. Thermo-physical Properties

Physical properties of adsorbent materials, such as their particle size distribution, porosity, permeability, density, specific heat capacity, surface area, pore volume distribution and thermal conductivity, have been shown to influence their adsorption uptake and kinetic capacity **[6, 17]**. The ability to

measure such properties is therefore necessary for the development of adsorbent materials and their applications as discussed below.

3.1 Particles size distribution and porosity

Powder porosity refers to the voids within the powder bed including spaces between agglomerates, between primary particles, and micro-spaces (micropores) within the particles. Powders with irregular shaped particles and anisometric particles (elongated or flattened shaped particles) have been reported to have more porosity than spherical shaped particles [18]. Powder porosity (ε) is correlated to powder bulk density as (porosity = 1 - (bulk density/true density)).

Particles with low density and high porosity have weaker interparticle Van der Waals forces. In contrast, powders with increased bulk densities and decreased porosities have higher cohesive forces due to the increase in the number of interparticle contacts. Particle porosity can be measured using mercury intrusion measurements **[20]**. The principle of this technique is based on the fact that mercury does not wet most substances and hence it will not penetrate pores by capillary action but must be forced into the pores by the application of external pressure. The required equilibrated pressure is inversely proportional to the pore size. Mercury porosimetry analysis is the progressive intrusion of mercury into a porous structure under stringently controlled pressures. The MIP instrument generates volume and size distributions from the

pressure versus intrusion data. Mercury porosimeter analysis is recommended for macroporous adsorbents. Gas adsorption is used for mesopores and micropores measurements where nitrogen or carbon dioxide is injected into the pores instead of mercury **[21]**.

Several techniques could be used to determine particle size distribution of adsorbent materials. For example, the sieving method employs several mesh sizes fitted placing the large meshes on top of the smaller mesh sizes. Each mesh holds adsorbent particles above a certain size. Following sieving, the weight of the powder held on top of each sieve size is recorded to get particle size distribution. In general, particle sieving is ideal for particles larger than 75 μm and is not suitable for particles smaller than 38 μm due to particle cohesiveness. Sieving could be performed wet or dry, by hand or by machine. Mechanical sieving is preferable for non-cohesive powders, whereas air-jet sieving is more suitable for cohesive powders [**22**]. In general, sieving results in particles larger than the sieve holes' diameters, especially for elongated particles.

Other techniques include scanning electron microscopy (SEM) [**23**], sedimentation methods, opto-electrical sensing, laser diffraction, and photon correlation spectroscopy. In SEM, a focused beam of high-energy electrons interacts with atoms in the sample, generating a variety of signals at the surface of the solid sample. The signals derived from electron-sample interactions

reveal much information including the particle size. Qualitative particle size determinations could be obtained by investigating an area having a particular number of particles and measuring the diameter by using the scale bar presented in the images. Sedimentation methods are based on the dispersion of the material particles in a liquid. Particles are allowed to settle and then the particle size is taken as a function of time. In the optical and electrical sensing zone method (Coulter Counter), electrical impedance (resistance) generates a voltage with an amplitude proportional to particle volumes in an electrolyte as they pass through an orifice. Laser diffraction methods use a laser beam that passes through a dispersed particulate sample, and the particle size distribution (ranging from 0.02 μm to 2000 μm) is measured from the angular variation in the intensity of the scattered light. Large particles scatter light at small angles relative to the laser beam and small particles scatter light at large angles. The angular scattering intensity data are analysed to calculate the size of the particles responsible for creating the scattering pattern. Finally, photon correlation spectroscopy (1 nm to 5 μm) measures the Brownian motion of fine particles as a function of time. A laser beam is scattered by particles in suspension. The diffusion of particles causes rapid fluctuations in scattering intensity around a mean value at a specified angle. From the scattered light intensity signal, information about the Brownian motion of the particles and subsequently their size is obtained. Laser diffraction does not take into account the apparent particle density and dynamic shape factors. Additionally, particles

with irregular surfaces result in high-angle scattering that could be interpreted as small particles. Therefore, the diffracted light can change with the orientation of non-spherical particles, and thus the results may not be a true representation of the actual size, especially for irregular shaped (e.g. elongated) particles. Possible alternatives include the use of size estimations obtained by SEM as discussed previously. Nevertheless, it should be acknowledged that laser diffraction gives volume-weighted size distribution estimations whereas SEM gives number-weighted size estimations. Table 1 summarizes the advantages and disadvantages of the foregoing techniques. Choosing a method for particle sizing depends on several factors such as the nature of the material to be sized, the estimated particle size distribution, the intended use, and cost.

3.2 Permeability

Permeability is an important characteristic for ensuring good refrigerant mass transfer through the packed adsorbent materials and the recommended permeability should be better than 10^{-12} m^2 **[24]**. Low permeability values result in high-pressure gradients and high mass-transfer resistance **[25]**. Usually, the experimental pressure drop and flow velocity are correlated with the permeability using the Darcy model **[26]** or Ergun model **[27]**. As velocities increase, discrepancies between experimental data and Darcy's law calculations appear; in such cases, the Ergun model would be more accurate. Increasing the

particle diameter increases the permeability but decreases the adsorption kinetics; there is an optimal particle diameter for the maximum cooling power output as given by Hongyu *et al*. **[28].** Experimental facilities for measuring the permeability typically use a differential pressure sensor and velocity measurement device as presented in Fig. 4.

3.3 True and bulk densities

The bulk density (or apparent density) is defined as the density of a large volume of porous material powder including the pore spaces within the material particles in the measurement volume. The bulk density can be measured using calibrated graduated cylinders filled with an accurately weighed specimen material **[20].**

True density (density of the pure solid material excluding both internal and external voids) is typically determined using a helium pycnometer. A defined volume of helium fills the pores in the chamber containing the sample, thus establishing their volume contribution in the measurement. Table 2 presents the bulk and true densities of activated carbon materials. True density measurements have been performed using a Quantachrome Ultrapyc 1200e helium pycnometer with vacuum purge option. Before analysis, the samples were cleared of contaminants (e.g. water) or trapped air by evacuation **[20]**. Bulk density is a powder characteristic whereas true density is a particle

characteristic. An activated carbon powder with a higher powder bulk density value indicates that there is a higher number of contact points between particles within this powder. A decreased bulk density for an activated carbon powder indicates that this powder has a higher specific surface area.

3.4 Specific heat

The specific heat is the amount of heat required to raise the temperature of unit mass of the sample by one degree Celsius. Highly conductive materials exhibit low specific heat capacity values. The specific heat capacity can be measured using differential scanning calorimetry (DSC) **[20]**. The measured heat flow is the product of the mass and specific heat capacity and heating rate, then the specific heat can be calculated using the previously measured stated parameters. For example, Table 2 presents DSC measurements conducted at a heating rate of 0.5 K/min with a maximum heating temperature of 130 ˚C. Adsorbent material heat capacity can be used to determine the effective specific heats of the adsorbent/refrigerant pair at different uptake values under isosteric conditions as shown by Eq. 1 **[29-31]**:

$$Cp_{eff} = C_{ads} + xC_{ref} \quad (1)$$

where C_{ref} is the refrigerant specific heat, C_{ads} is the adsorbent specific heat and x is the adsorption capacity in kg/kg.

3.5 Surface area and pore volume distribution

Surface characteristics such as surface area, pore size and volume of any material refer to the properties associated with its surface geometry and may ultimately determine its uptake. A range of different methods is used to measure the various surface properties. Many methods are based on the isothermal adsorption of nitrogen. The surface area of porous materials is usually measured either according to the Langmuir's theory or Brunauer Emmet and Teller (BET) theory.

The Langmuir model is based on the maximum amount of adsorbate (usually nitrogen) adsorbed per gram of adsorbent for the formation of a monolayer. The molecular weight of the adsorbate and knowledge of the approximate contact area of an adsorbate molecule facilitate the determination of surface area of adsorbent. The most common and reliable BET method employs the adsorption of nitrogen, CO_2, argon or krypton on the adsorbent samples [**20**]. The BET equation is used to give the volume of gas needed to form a monolayer on the surface of the sample. The actual surface area can be then calculated using the size and the number of the adsorbed gas molecules. The Langmuir surface area is always higher than the BET surface area, as the Langmuir equation considers the monolayer as the limit of adsorption while the BET equation is based on the concept of multilayer adsorption with regards to the monolayer. Other, less commonly used, methods for determining the surface area have been presented including the free surface energy method of Fu and Bartell and the uniform

circular capillaries method **[32]**. In this method, samples are pretreated by applying some combination of heat, vacuum, and/or flowing gas to remove adsorbed contaminants acquired (typically water and carbon dioxide) from atmospheric exposure. The solid is then cooled, under vacuum, usually to cryogenic temperatures (77 K, -195 ^{o}C). An adsorptive (typically nitrogen) is dosed to the solid in controlled increments. After each dose of adsorptive, the pressure is allowed to equilibrate and the quantity adsorbed is calculated. The quantity adsorbed at each pressure (and temperature) defines an adsorption isotherm, from which the quantity of gas required to form a monolayer over the external surface of the solid is determined; with the area covered by each adsorbed gas molecule known, the surface area can be calculated.

Powder specific surface area has been related to particle size distribution, surface energy, surface roughness, bulk density, crystallinity, and electrostatic charge. Particles with a higher surface area show higher moisture uptake [33]. The surface area also depends on the size of the pores, which can be measured using the density functional theory (DFT) where the pore size can be determined by the observed peaks in the pore size distribution **[20]** as presented in Fig. 5. In this figure, two peaks are observed: the first one is for the small pore width 0.32 nm while the second peak is related to the large pores with width 0.5-0.7 nm. Such volume distribution can be linked to the adsorption capacity of the material where the pore size affects its adsorption ability for a

particular refrigerant **[20]**. For example, methanol is better adsorbed by activated carbon compared to silica gel where activated carbon pore size is dominated by pores less than 2 nm while the silica gel includes a wider range of micro and mesopores as shown in Fig. 6.

3.6 Thermal conductivity

Thermal conductivity is an indication of the degree to which a material can conduct heat. It describes the transport of energy in the form of heat through a body as the result of a temperature gradient. It is a crucial parameter as it controls the heat transfer to the adsorbent materials during the adsorption and desorption phases and the operating cycle time.

Thermal conductivity is determined either using steady-state or transient techniques. The transient technique is more suitable for adsorbent materials to take into account the short cycle time used in adsorption cooling applications. The development of experimental facilities that can measure the thermal conductivity of dry adsorbent are reported in Çağlar **[34]**, while measurements of wet adsorbent under vacuum are reported by Wang *et al*. **[35]**, Dawoud *et al*. (using 4A zeolite/water with thermal conductivity less than 0.26 W/m.K) **[36]**, Freni *et al*. (water /composite SWS achieving conductivity of 0.2-0.3 W/m.K) **[37]** and Gurgel *et al*. **[38]**. In the dry measurement approach, an effective thermal conductivity model should be used to combine the adsorbent and refrigerant conductivities. The facilities for measuring the conductivity of dry

adsorbents include infrared detectors as used by Zhao *et al*. **[29]**, Jiang *et al*. **[39]** and Zhao *et al*. **[40]** and shown in Fig. 7; and transient plane source methods (TPS) as used by Hu *et al*. **[41]**. An infrared detector is used to measure the corresponding temperature rise of the sample due to timed exposure to laser light on the surface; the increment of temperature versus time curve can then be drawn. The thermal diffusivity is determined by thickness of the testing samples and time required for raising the sample temperature (thermal conductivity = calculated thermal diffusivity x sample specific heat x sample density). The Transient Plane Source technique typically employs two sample halves, in-between which the sensor is sandwiched. Normally the samples should be homogeneous. During the measurement, a constant electrical effect passes through the conducting spiral, increasing the sensor temperature. By recording temperature with time response of the sensor (the mean temperature change of the sensor is defined in terms of the dimensionless variable of time and thermal diffusivity), the thermal diffusivity and thermal conductivity of the material can be calculated. The conductivity (expressed in terms of measured heat flux and adsorbent thickness, following Fourier's law **[5]**) of wet adsorbent material using a hot wire method (with refrigerant under vacuum (Fig. 8) depends on both the operating temperatures and pressures. Measuring the thermal conductivity through the wet approach is more desirable and accurate compared to the dry method as the latter approach requires assumptions of mixing rules, such as those described by Maxwell-Eucken,

between the refrigerant and the solid material. Such assumptions may lead to a degree of uncertainty in the effective adsorption bed thermal conductivity.

4. Adsorption characteristics

This section discusses the current techniques used to measure material performance, including isotherms and kinetics. The major parameters that influence the performance of adsorbent materials are capacity, selectivity, ability to regenerate, kinetics, cost, and the minimum regeneration temperature of an available heat source **[6]**.

Many refrigerants have been used with activated carbon materials in adsorption systems research, including ammonia, methanol, ethanol, carbon dioxide (Table 3). Ammonia has a large latent heat of vapourization tested with activated carbon **[30, 63]** or composites **[64]** adsorbents. It has been shown to work at low temperature in ice makers but it is flammable and toxic. Hydrocarbons such as butane and propane have been investigated by many researchers [**30,65**]. The main disadvantages of hydrocarbons are their low latent heat and modest uptake which makes their performance very low and unattractive for adsorption systems. Methanol has a good latent heat (1224 kJ/kg) and methanol/activated carbon uptake is nearly twice that of water/silica gel resulting in similar cooling capacity **[66]**. Ethanol has moderate latent heat,

nearly three times than that of HFC134a, Carbon dioxide, butane, and propane and nearly 80% that of methanol. It is non-toxic and flammable but operates under desorption temperatures lower than 120 °C without problems regarding flammability. Although carbon dioxide is natural, non-toxic, non-flammable, it has a very high operating pressure that can be up to 7 MPa. Much of the existing published literature on the use of carbon dioxide is related to developing adsorption isotherms **[67-69]** or theoretical cycle analysis **[70]**. Pressure swing adsorption cooling has been accomplished using carbon dioxide and activated carbon by Anupam *et al*. **[71]**, achieving lower temperatures below 0 °C with a large number of cycles (compression combined with adsorption, bed cooling, desorption combined with expansion). Although HFC134a has been investigated by many authors **[72-74]**, it has high global warming potential (GWP) that will restrict its future usage. Ramji **[55]** compared the trend of chilled fluid temperatures of different refrigerants with the same kind of activated carbon as shown in Fig. 9.

Several authors tested pure refrigerants, hydrocarbons and refrigerant blends. Ismail *et al*. [42] tested Maxsorb III with several refrigerants: R32, R507, R290, and R134a. They concluded that R-32 produced the highest specific cooling capacities at high chilling and low ambient temperatures. Attalla *et al*. [43] measured the Granular GAC/R134a performance in circular tube heat exchanger adsorber with fins. Measurements showed that large uptake of R134a

(up to 1.92) was observed with GAC activated carbon after 1200 sec. Shmroukh *et al*. [51,52] tested several activated adsorbents in both granular and powder forms, i.e. R-134a, R-407c, R-507A. Measurements showed that ACP/R-134a pair is highly recommended for use as an adsorption refrigeration working pair because of its higher maximum adsorption capacity compared to other tested pairs. Habib *et al*. [54] simulated an 8 kW unit with AC/R134a. A single-stage chiller was superior when the heat source temperature was relatively higher (above 75˚C), however, when the regeneration temperature was at or below 55˚C, the two-stage chiller would still operate. Ramji *et al*. [55] tested water/ammonia/methanol with activated carbons. Their simulations showed activated carbon-water pair to yield the highest COP of 0.58 due to the high heat of evaporation. Habib *et al*. [56] investigated the adsorption uptakes of ACF/Ethanol, AC/Methanol and water/silica gel. ACF/ethanol showed the highest adsorption uptake followed by AC-methanol and silica gel-water pairs. Silica gel-water showed the highest COP value of 0.5 when the regeneration temperature was below 70 °C; however, the COP of the ACF-ethanol based adsorption cycle was found to be the highest when the regeneration temperature was above 70 °C. Jribi *et al*. [57] simulated a novel CO_2 / Maxsorb III adsorption chiller with 1.72 kW of cooling power at a driving heat source temperature of 85 °C and with 80 kg of adsorbent. Further to his investigation, the author investigated **[58]** a new pair AC/HFO1234ze(E) as an alternative of AC/R134a with slightly better performance (COP of 0.15) at low regeneration

temperatures of 70 °C. Askalany *et al*. **[61-62]** investigated Maxsorb III and ACF with R410A and R32, respectively. Maxsorb uptake capacity (up to 1.8 kg/kg_{ads}) was higher by 1.6 times than that of ACF.

Other authors focused their testing and simulations on ethanol and methanol activated carbons. Miyazaki *et al*. **[44]** investigated chemically treated Maxsorb/Ethanol and recommended that the time length of the adsorption process should be longer than that of the desorption process for the maximum SCP. An SCP of 140 W/kg with COP of 0.48 was predicted by simulation with the temperature conditions of 80 $^{\circ}C$ for hot water, 30 $^{\circ}C$ for cooling water, and 14 $^{\circ}C$ for chilled water. Habib and Saha **[45]** simulated AC fibre ACF-20/ethanol pair in a lumped analysis for an adsorption chiller driven by solar energy for the hot climate of Malaysia. Chekirou *et al*. **[46]** tested AC-35/Methanol in a solar cooling system and found that the optimal thermal performance coefficient COP_{th} was achieved at internal adsorber radius R2 of 60 mm. Rowe KC **[47]** simulated a 4-bed chiller with AC-35/Methanol with COP of 0.33 and SCP of 327 W/kg. Phenol resin based activated carbons were found to adsorb up to 1.2 $kg_{ethanol}/kg_{ads}$ as reported in Jerai *et al*. [48]. Hassan [49] developed a simulation model for a refrigerator performing at a COP of 0.6 for AC/Methanol pair. Multi-cycle using zeolite and activated carbon in the upper cycle developed by He *et al*. [50] reported a COP of 0.4. Umair *et al*. [53] simulated the performance of activated carbon fibre/Ethanol for a solar cooling refrigerator. Uddin *et al*. [59] and El-Sharkawy *et al*. [60] tested different

versions of chemically modified activated carbons with ethanol. The adsorption capacity of H2 treated Maxsorb III/ethanol was slightly higher than that of the parent Maxsorb III/ethanol pair while the $KOHeH_2$ treated Maxsorb III showed the lowest adsorption capacity.

A review of the recent literature reveals that ethanol/modified activated carbon for low cooling temperature applications is a popular focus of research, mainly due to the non-toxicity, low-flammability, and environmentally benign nature of ethanol. A number of such modified activated carbon materials have uptakes approaching 1.2 $kg_{ethanol}/kg_{adsorbent}$ [48, 59, 60].

4.1 Adsorption isotherms

A range of experimental methods is used to determine adsorbent material isotherms including gas flow, volumetric, and gravimetric methods **[75, 76]**.

In the gas flow technique, helium is used as the carrier gas and the partial pressure of adsorbate is determined by the gas flow meter. The volume adsorbed by the adsorbent is determined from the peak area in the adsorption/desorption chart recorded over time by a potentiometer. This apparatus is simple, inexpensive, easy to handle, requires no vacuum, and available gas chromatographers can also be modified for this approach. However, the measurement of the adsorbed amount is indirect and the method does not claim high precision.

In the volumetric technique, the adsorbent is placed in an evacuated chamber and the charging chamber includes the initial charge of refrigerant. Regulating flow between two chambers and the application of the ideal gas can be used to determine both kinetic and equilibrium adsorption isotherms as presented in Fig. 10. The volumetric method has the advantage of simplicity of design and cost effectiveness. Disadvantages of the volumetric method include:

i. Several grams of sorbent material are needed for the volumetric measurements because only considerable changes in the gas pressure, caused by adsorption, can be observed. If only tiny amounts (e.g. several milligrams) of the sorbent are available gravimetric measurements are then strongly recommended.

ii. Gas adsorption processes may last for various times according to the adsorbent material. Therefore, one can never be certain that equilibrium in a volumetric experiment has been realized unless control and alarm units are utilized to check the adsorption process condition.

iii. The hot dry sample weight could have some uncertainties during handling and packing of adsorbent inside the bed, although this uncertainty is usually less than 1%.

In gravimetric techniques, the weight of a sample is measured by a microbalance located inside a vacuum system and isolated from the surroundings. A furnace heats the sample. The gas can be purged into the

system, and then adsorption occurs. The balance measures the weight change of adsorbent directly as illustrated in Fig. 11. Isotherms can be obtained directly at different pressures and temperatures. The gravimetric method has the following advantages in comparison to the volumetric methods.

i. Microbalances commonly exhibit high reproducibility, sensitivity, and accuracy, hence they allow an accurate determination of the adsorbed gas masses.

ii. For highly sensitive microbalances (e.g., Thermo Cahn, Hiden, Mettler Toledo, Rubotherm, Setaram, TA Instruments, VTI) only tiny amounts of sorbent materials are needed to measure gas adsorption equilibria.

iii. Microbalances with a data recording system allow one to observe the process of approaching equilibrium. Such measurements deliver information concerning the kinetics of the adsorption process.

iv. Contrary to the volumetric method, very high and very low pressures of the sorptive gas can be accommodated in gravimetric measurements.

v. Modern microbalances allow recoding weight data every tenth of a second. If the kinetics of a pure gas sorption process is slow compared to this time, it can be easily recorded.

vi. In practice, the activation of a sorbent material can be accomplished more easily in gravimetric sorption instruments compared to other instruments.

In gravimetric methods, the mass of the sample can be recorded during the activation process.

Disadvantages of the gravimetric approach include:

i. Complexity where modern microbalances, especially the magnetic suspension balances, are used. These devices are complex systems in their design and regular maintenance may thus be needed.

ii. Oscillations of the microbalance caused by external vibrations e.g. road traffic. Also, fine grained sorbent materials, especially activated carbon fibres or powder, may cause problems as they may change their position within a vessel mounted to the balance or may simply be blown out of the vessel due to the sorptive gas flow.

iii. In the case of the low-temperature measurements, such as those using liquid nitrogen (77 K), it is difficult to maintain temperature stability. Accordingly, the gravimetric method is commonly used at or above room temperature.

iv. Mixture adsorption processes normally cannot be detected by simple gravimetric measurements. This is because the sorptive gas mixture must be circulated during the process to avoid local concentration gradients. As the gas flow inside the adsorption vessel causes dynamic forces acting on the sorbent sample, the balance recording is changed.

Isotherm data of different pairs were measured at different operating temperatures and pressures for various activated carbons pairs **[12, 77, 78, 79]**. El-Sharkawy *et al*. **[12]** tested ethanol/Maxsorb III with 72 micron mean particle diameter using a TGA reacting chamber shown in Fig. 12. The data were generated at an evaporation temperature of 15 °C and adsorption temperature range of 20-60 ^{o}C. Cui *et al*. **[77]** developed the isotherm for the composite adsorbent at 27 °C evaporating temperature using a high-vacuum gravimetric method. Ivanova *et al*. **[78]** tested ethanol treated zeolite with HCl solutions for concentrations up to 3%. Activated carbon fibre (A-20) and (A-15) isotherms were developed by El-Sharkawy *et al*. **[79]** through a specially designed apparatus where the amount of ethanol adsorbed at the equilibrium condition and the refrigerant level inside the evaporator were measured using a digital microscope with ± 0.01 mm resolution prior to and after each experiment. The mass of ethanol evaporated was calculated using the liquid level difference.

4.2 Adsorption kinetics

Numerous different techniques are available for the recording of adsorbed/desorbed mass transfer rates, including gravimetric, calorimetric, volumetric, and micro-flow controller techniques. In the gravimetric technique, the mass of adsorbent is measured directly using a microbalance with the adsorbate synchronised with the adsorption process. The gravimetric method

has been used in measuring the adsorption kinetics of ethanol onto eleven commercially available activated carbon species [80]. An electronic balance has also been used for the kinetics of water/composite adsorbent pairs which were synthesized from activated carbon, silica gel and $CaCl_2$ [51]. Other methods have been reported which determine the weight of the bed by load cell with water/SAPO-34 pair [81, 82] where a voltage sensor output signal is calibrated against weight.

The calorimetric concept relates the measured heat rate released due to the adsorption process to the mass adsorbed using thermoelectric devices. This concept has been used in many cases such as in the case of water adsorption on type A beaded silica gel particles bonded to aluminium [83]. A heat flux sensor is used in a calorimeter where water is adsorbed on a layer of zeolite (UOP DDZ 70) [84] or micro-calorimetric sensor using a Tian–Calvet-type micro-calorimeter where water vapour is adsorbed on silica gel.

In the volumetric method, the refrigerant is charged in a charging chamber and is recorded by several techniques, including recording of the liquid level using a digital microscope as ethanol is adsorbed onto Unitika activated carbon fibre (ACF) of types (A-20) and (A-15) [3]. Another method using a magnetostrictive level sensor has been employed for many working pairs such as activated carbon–methanol, activated carbon–ammonia, and composite adsorbent–ammonia [86]. The sensor incorporates a float sending magnetic

signals to the sensor end which outputs current or voltage in response to the liquid refrigerant level.

Other investigators have utilized manual recording of the height level using a graduated transparent glass vessel such as that presented in [87-90] where ammonia is adsorbed on $BaCl_2$ impregnated into a vermiculite matrix. Other concepts used include those based on expressing the liquid level as a function of the pressure difference of the liquid such as in the adsorption of ammonia on six samples of three types of adsorbents (consolidated AC with expanded natural graphite treated with sulfuric acid (ENG-TSA), consolidated AC with expanded natural graphite (ENG) and granular AC) with different densities and different grain sizes reported in [29]. Pressure readings were converted into pressure heads, which are used to express the adsorbed mass by converting the refrigerant level difference in a liquid column before and after adsorption into liquid volume which is multiplied by the liquid refrigerant density to determine the adsorbed refrigerant mass.

In the constant volume variable pressure method, which has been used with AC/HFC134a and AC/HFC507a pairs, the mass of initial charge is measured and the mass transferred to the adsorbent chamber, which is tracked by pressure and temperature measurements and an equation of state [91].

In the large temperature jump method, the adsorption process is a simulation of the non-isothermal adsorption/desorption process such as

adsorbed water vapour on pellets of composite sorbent SWS-1L ($CaCl_2$ in silica KSK) placed on a metal plate as presented by Aristov [92]. The kinetics are measured under simulated conditions similar to the real adsorption chiller operation where the sample is tested under an initial high temperature then suddenly cooled or reversed in condition.

The micro-flow controller technique measures the flow rate of desorbed/adsorbed mass, and the integration of the flow rate over a period of time gives the refrigerant uptake such as composite adsorbents synthesized from zeolite 13X and $CaCl_2$/water vapour pairs tested in [68, 93]. Figures 13 to 16 present examples of these techniques. It should be mentioned that some of the presented techniques are conducted with only a few milligrams of a solid adsorbent such as microbalance techniques with 10 mg [80] or the heat flux sensor method introduced by Füldner [84]. Characterization of materials from tiny material quantity makes such techniques suitable for the characterization of expensive materials such as metal-organic framework (MOF) materials. Other techniques mostly employ volumetric methods and require larger material quantities, ranging from few grams to kilograms, e.g. load cell with 42 g [81] and up to 600 g [82].

5. Adsorption cooling system analysis and modelling techniques

Modelling of adsorption cooling systems is a very effective tool in the design and performance optimization of such systems. There are many

modelling techniques used to model adsorption cooling systems such as the lumped analysis [95-103] and the distributed-parameter simulation technique [104] where variations in uptake and temperature with space directions are taken into consideration. Recent advances in computers power and computational techniques, such as computational fluid dynamics (CFD), can solve heat, and mass transfer problems to obtain temperature distribution, velocity, pressure and refrigerant concentration levels in both transient and steady states, and can thus facilitate optimization the bed design of adsorption cooling systems [105-107].

5.1Modelling of Adsorbent materials

For adsorbent materials, modelling the adsorption characteristics is necessary for designing an efficient adsorption system. For adsorption isotherms, Aristov **[108]** correlated the material uptake in terms of sorption free energy (ΔF) [J/mol], in the following form:

$$x^*(\Delta F) = a + b\Delta F + c\Delta F^2 + ... \quad (2)$$

where x^* is the equilibrium uptake and a,b,c are empirical constants found from fitting to experimental data. The Polanyi potential theory considers the adsorption process to be similar to that of condensation, and the adsorbed refrigerant state to behave like a liquid [108]. In this approach, complex isotherms can be recorded by dividing the isotherm into multiple curves with its own fitted constant in the mathematical form described in the above equation.

In 1916, Langmuir presented an isotherm model for gas adsorption onto solids [109]. It is a semi-empirical isotherm model derived from a proposed kinetic mechanism. The Langmuir model was originally developed to represent the behavior of monolayer adsorption [108]. The model is based on four assumptions:

1) Uniform surface of the adsorbent where all the adsorption sites are equivalent.
2) There is no interaction between the adsorbent molecules.
3) All adsorption occurs by the same mechanism.
4) At maximum loading, only a monolayer is formed: molecules of adsorbate do not deposit on other, already adsorbed, molecules of adsorbate, only on the free surface of the adsorbent. This model is expressed as;

$$\frac{x^*}{x_0} = \frac{bP}{1+bP} \tag{3}$$

in which,

$$b = b_0 e^{(\frac{\Delta H_{ads}}{RT})} \tag{4}$$

where

x_0 is an empirical constant that represents the maximum adsorption capacity in kg/kg, b_0 is adsorption affinity at infinite temperature in 1/kPa, P is the bed pressure [kPa], ΔH_{ads} is the isosteric heat of adsorption in kJ/kg, R is the gas constant in kJ/kg and T is the temperature in K. The Langmuir equation has been modified by Tóth using a fitting parameter (t). The Toth equation contains

three fitting parameters, as a result it describes well many adsorption data for practical adsorbents. This model is expressed in Eq. 5 [110].

$$\frac{x^*}{x_0} = \frac{bP}{\left(1+\left(bP\right)^m\right)^{1/m}} \tag{5}$$

$$b = b_0 e^{\left(\frac{\Delta H_{ads}}{RT}\right)} \tag{6}$$

where m is empirical constant determined from fitting the isotherm data. When t is equal to 1, the equation reduces to the Langmuir equation [75].

The Dubinin–Astakhov (D-A) was reported as the most representative model for activated carbon adsorption [12,111]. The model has been developed mainly to describe the adsorption of gases in microporous adsorbents and is particularly appropriate for activated carbon with a large pore heterogeneousness. The heterogeneity coefficient (n) in such a model provides greater flexibility in fitting of the experimental isotherms compared to Dubinin–Radushkevich in which the heterogeneity coefficient is fixed to a value of 2. The heterogeneity coefficient takes the effect of non-uniform pore sizes on the surface (n = 2) in the case of homogenous pore sizes **[112]**. The greater the value of the heterogeneity coefficient of a working pair, the higher the regeneration temperature required to release the refrigerant.

$$x^* = x_0 \exp\left(-\left(\frac{\Delta F}{E}\right)^n\right) \tag{7}$$

where x_o [kg/kg], n, E [J/mol] are the empirical constants obtained from fitting isotherm experimental data.

Usually, Langmuir and Dubinin–Astakhov (at high and low partial pressure ratios) models fail to predict the isotherms of mesoporous heterogeneous surfaces similar to water/silica gel [113]. The Langmuir model has limitations in fitting uptake data at high pressure and in the case of heterogeneous materials. Alternatively, the Tóth model is commonly used for heterogeneous adsorbents such as activated carbon because of its ability to more realistically represent behavior at both the low and high pressures. Dubinin and Astakhov proposed their model for adsorption of vapours and gases onto non-homogeneous carbonaceous solids with wider pore size distributions [118].

The adsorption isotherms can be used to determine the heat of adsorption as shown in the following equation [108]:

$$\Delta H_{ads} = -R\frac{\partial \ln P}{\left(\partial\left(1/T\right)\right)} = -R\frac{\ln P_2 - \ln P_1}{\left(1/T_2 - 1/T_1\right)} \quad (8)$$

T_1 [K] and T_2 [K] are two different operating points of the bed temperature on the same isosteric lines. For adsorption kinetics, several models are available in the literature to track the adsorption rate with time. The most commonly used model is the linear driving force (LDF) model. El-Sharkawy *et al*. **[114]** predicted the adsorption uptake using the modified LDF model to account for

both micropores and mesopores of the adsorbent materials that are described as follows:

$$\frac{dx}{dt} = \frac{F_o D_s}{R_p^2}(x^* - x) \tag{9}$$

where x^*, x, R_p represent the volume averaged equilibrium uptake after a long time, the volume averaged instantaneous uptake, and particle radius respectively. F_o is the particle geometry constant and D_s is the surface diffusion coefficient [m^2/s]. Other investigators utilized the particle diffusion approach by incorporating a Fickian model **[78, 91]** with analytical solutions as presented in Eq. 10:

$$\frac{x - x_{in}}{x^* - x_{in}} = 1 - \frac{6}{\pi^2}\sum_{n=1}^{\infty}\frac{1}{n^2}\exp\left(\frac{-n^2\pi^2 D_s t}{R_p^2}\right) \tag{10}$$

where x_{in} is the initial uptake of the adsorbent sample and n varying (1 to ∞). Constant 6 is for spherically shaped adsorbents.

5.2 CFD modelling of adsorption processes

Two CFD approaches are commonly used for simulating adsorption beds. The first approach is based on modelling the adsorbent material as a solid volume with porosity, whereas the second approach models the adsorbent material as physical particles and solves heat and mass transfer equations for each of these particles **[105]**. In the first approach, Sahoo *et al*. **[25]** used equations Eqs.11 to 15 to model an activated carbon adsorption bed used for methane storage.

$$\frac{\partial\left(\varepsilon\rho_g + \rho_b x\right)}{\partial t} + \nabla \bullet \left(\rho_g u_g\right) = 0 \tag{11}$$

$$\frac{\rho_g}{\varepsilon}\frac{\partial u_g}{\partial t} + \frac{\rho_g}{\varepsilon^2} u_g \bullet \nabla u_g = -\nabla P + \mu_g \nabla^2 u_g - \frac{\mu_g}{K} u_g \tag{12}$$

$$\left(\rho c\right)_{eff}\frac{\partial T}{\partial T} + \rho_g C_{p,g} u_g \bullet \nabla T = \nabla \bullet \left(\lambda_{eff} \nabla T\right) + \rho_b \Delta H_{ads}\frac{\partial x}{\partial t} \tag{13}$$

where ρ_b is the bulk bed density ρ_g is the vapour density, u_g is the vapour velocity in the bed, ε is the bed porosity, t represents the time, ∇P is the pressure gradient, ∇T is the temperature gradient. K is the bed permeability, C_p is the specific heat, and λ_{eff} is effective thermal conductivity of adsorbent/vapour porous material. Neglecting the unsteady, drag and viscous terms, the momentum equation (12) reduces to the Darcy form as:

$$u_g = -\frac{K}{\mu_g}\nabla P \tag{14}$$

where the permeability K was calculated from:

$$K = \frac{d_p^2 \varepsilon^3}{150\left(1-\varepsilon\right)^2} \tag{15}$$

where d_p is the particle size [m], The effective specific heat and thermal conductivity values were calculated as:

$$\left(\rho c\right)_{eff} = \left(\varepsilon\rho_g + \rho_b x\right)C_{p,g} + \left(1-\varepsilon\right)\rho_s C_{p,s} \tag{16}$$

$$\rho_b = \left(1-\varepsilon\right)\rho_s \tag{17}$$

$$\lambda_{eff} = \varepsilon\lambda_g + \lambda_s(1-\varepsilon) \quad (18)$$

where ρ_b and ρ_s are the packing and solid carbon densities.

Elsayed *et al*. [80] used the above CFD model with a modified thermal conductivity equation (Eq. 19) to simulate a flat plate adsorber bed packed with Maxsorb activated carbon/cooling water on the sides of plate exchanger (shown schematically in Fig. 17) with instantaneous uptake calculated from LDF model in the governing equations.

$$\lambda_{eff} = \lambda_s \frac{2\lambda_s + \lambda_g - 2\varepsilon(\lambda_s - \lambda_g)}{2\lambda_s + \lambda_g + \varepsilon(\lambda_s - \lambda_g)} \quad (19)$$

where λ_s and λ_g are the solid adsorbent and refrigerant vapour thermal conductivities.

The adsorbent layer thickness affects the size, cooling capacity and energy efficiency of adsorption machine. The amount of adsorbed refrigerant equals to the refrigerant uptake multiplied by the amount of the packed adsorbent material. As the adsorbent layer thickness increases, the mass of adsorbent material increases but the refrigerant uptake decreases due to the reduction in the bed permeability and the reduction in the effectiveness of cooling the adsorbent material. Fig. 18 presents the variation of specific cooling power of Maxsorb with time for various layer thicknesses. The use of large layer thicknesses reduces the specific cooling power significantly as the SCP decreased from 45 W/kg to 14 W/kg by increasing the packing depth from 5 mm to 20 mm. It should be noted that the Darcy approach is accurate only in

cases where the velocity of vapour is low and where drag and viscous effects are negligible. Regarding the second CFD approach, Füldner and Schnable **[84]** used equations 20 to 23 to model the diffusion process inside a thin layer of zeolite adsorbent material.

$$\frac{\partial c}{\partial t} - \nabla \cdot (D_{eff} \nabla c) = -\frac{\rho_b}{M \varepsilon} \frac{\partial x}{\partial t} \tag{20}$$

where C is the refrigerant concentration mol/m^3 and D_{eff} is the effective diffusivity [m^2/s].

Instead of using LDF model, the instantaneous uptake is directly related to temperature and pressure change:

$$\frac{\partial x}{\partial t} = \left(\frac{\partial x}{\partial T} \right)_{p=const} \frac{\partial T}{\partial t} + \left(\frac{\partial x}{\partial p} \right)_{T=const} \frac{\partial p}{\partial t} \tag{21}$$

where the pressure is related to concentration using ideal gas relations:

$$p = C * R_{universal} * T \tag{22}$$

The energy equation expressed by combining equations 21 and 22:

$$\left(\rho Cp\right)_{eff} \frac{\partial T}{\partial t} = \nabla \cdot \left(\lambda_{eff} \nabla T\right) + \rho_b \Delta H_{ad\,s} \frac{\partial x}{\partial t} - \rho_b Cp_g x \frac{dT}{dt} \tag{23}$$

Freni *et al*. **[105]** used the same equations to simulate water vapour/silica gel granule adsorption where the effect of packing depth on the uptake and temperature distribution was investigated as shown in Fig. 19. Elsayed *et al*.

[107] used the same technique to simulate ethanol/Norit RX3 pellet adsorption as presented in Fig. 20. In the work of the previous authors, except Füldner and Schnable, the effect of interparticle resistance was neglected (mass transfer resistance in the vapour surrounding the particles i.e., constant pressure boundary conditions over bed surfaces were utilized). Such conditions of uniform pressure may not be satisfied if there was no good transfer of vapour from adsorber bed to evaporator/condenser [115, 116] as the pressure may be elevated in the bed during desorption process and desorber pressure starts to become higher than the condensation pressure. Such simplified assumptions could over-predict the uptake with adsorption process or under-predict the uptake with desorption operation as the pressure gradient between the vapour and particle surface was neglected by assuming no interparticle resistance. Recent research by Niazmand *et al*. [116] considered the diffusion effects in the bulk vapour where the optimal particle size was investigated. The use of particles with a smaller size results in faster adsorption kinetics but it reduces the bed permeability due to decreased interparticle voids. It should be mentioned that although this type of mathematical model is highly detailed, it requires significant computing time and resources. Regarding the diffusion resistance in the porous solid particle, the LDF model was found to be as accurate as the diffusion models in cases with a diffusion ratio ($D/(r^2.t_{ads})$) of more than 0.3, as clarified by Hong *et al*. [117].

6 Conclusions

The appropriate measurement of adsorption properties is a critical component in the investigation of new adsorption pairs and in the optimization of adsorption applications. Existing techniques for the measurement of these properties have been reviewed. The adsorption characteristics were classified into thermo-physical properties and adsorption characteristics. The thermo-physical properties include particle size, sample porosity, permeability, true density, bulk density, specific heat, surface area, pore volume distribution and thermal conductivity. The techniques employed to experimentally measure the adsorption characteristics including adsorption isotherms and kinetics were discussed. Techniques of measuring kinetics were identified for the measurement of the performance of expensive materials where samples of only a few milligrams can be used. A range of equations was identified for the modelling of the adsorption characteristics, most notably, Langmuir, Tóth and Dubinin–Astakhov equations. LDF and Fickian equations have been used to model the adsorption kinetics. Additionally, CFD models used in the simulation of adsorption cooling systems were reviewed. The selection of kinetics techniques can be optimized based on cost and target sample to be measured.

The linear driving force model was extensively utilized by researchers due to its ease of mathematical representation and reduced computational time taken to predict the adsorption kinetics. However, under circumstance where

there is difficulty of transporting the vapour between the bed and evaporator/condenser, such as bed designs with small gaps between packed bed and chamber walls that result in a large pressure differences between the adsorption bed and evaporator/condenser, it is desirable to utilize a diffusion model to record the local variation in vapour pressure close to porous solid particles.

Chemically modified activated carbon surfaces represent a promising candidate for future applications, however further research is needed in the future to test such materials in full-scale adsorption units and to develop more efficient materials that are cost-effective in large quantities.

References

[1] Tamainot -Telto, Z, Critoph, RE. Adsorption refrigerator using monolithic carbon-ammonia pair. lnt J Refrig 1996; 20(2): 146-155.

[2] Meunier F. Second law analysis of a solid adsorption heat pump operating on reversible cascade cycles: application to the zeolite-water pair. Heat Recovery Syst 1985; **5**(2): 133-141.

[3] El-Sharkawy II, Kuwahara K, Saha BB, Koyama S, Ng KC. Experimental investigation of activated carbon fibers/ethanol pairs for adsorption cooling system application. Appl Therm Eng 2006; 26(8-9):859–865.

[4] Yeo THC., Tan IAW, Abdullah MO. Development of adsorption air-conditioning technology using modified activated carbon – A review. Renew Sustain Energy Rev, 2012; 16(5):3355– 3363.

[5] Wang K, Wu JY, Wang, RZ, Wang LW. Effective thermal conductivity of expanded graphite–$CaCl_2$ composite adsorbent for chemical adsorption chillers. Energy Convers Manage 2006; 47(13–14):1902–1912.

[6] Yang RT. Adsorbents: fundamentals and applications. John Wiley & Sons, 2003.

[7] Aristov Y. Novel Materials for adsorptive heat pumping and storage: Screening and nanotailoring of sorption properties. J Chem Eng Jpn 2007; 40(13): 1242-1251.

[8] Bansal RC, Goyal M. Activated Carbon Adsorption. Taylor & Francis Group, 2005.

[9] Lartey RB, Francis A. Developing national capability for manufacture of activated carbon from agricultural wastes. Institute of Industrial Research, *CSIR*, 1999, *Accra*, Ghana . from: http://www.africantechnologyforum.org/GhIE/ActCarbon.htm

[10] Spahis N, Addoun A, Mahmoudi H. Study on solar adsorption refrigeration cycle utilizing activated carbon prepared from olive stones. Revue des Energies Renouvelables 2007; 10(3): 415 – 420.

[11] Abdullah M O, Tan, IAW, Limb LS. Automobile adsorption air-conditioning system using oil palm biomass-based activated carbon: A review. Renewable Sustainable Energy Rev 2011; **15**(4): 2061–2072.

[12] El-Sharkawy II, Saha BB, Koyama S, He J, Yap KC & Ng C. Experimental investigation on activated carbon–ethanol pair for solar powered adsorption cooling applications. Int. J Refrig 2008; 31(8),:1407 -1413.

[13] Askalany A, Salem M, Ismail IM, Ali AHH, Morsy MG. Experimental study on adsorption-desorption characteristics of granular activated carbon/R134a pair. Int J Refrig 2012; 35: 494 -498.

[14] Zhong Y, Critoph RE, Thorpe R. Evaluation of the performance of solid sorption refrigeration systems using carbon dioxide as refrigerant. Appl Therm Eng 2006; 26(16): 1807–1811.

[15] El-Sharkawy II, Hassan M, Saha BB, Koyama S, Nasr MM. Study on adsorption of methanol onto carbon based adsorbents. Int J Refrig 2009; ***32***(7): 1579–1586.

[16] Ullah KR, Saidur R, Ping HW, Akikur RK, Shuvo NH. A review of solar thermal refrigeration and cooling methods. Renew Sustain Energy Rev 2013; **24**: 499–513.

[17] Królicki, Z, Wilk T, Zajączkowski B, Kaczmarczyk J. Research on adsorption characteristics of active carbon and silica gel and application in solar refrigeration and heat pump.*61st ATI National Congress –International Session "Solar Heating and Cooling"*, 2006.

[18] Kaialy W, Alhalaweh A, Velaga, SP, Nokhodchi, A. Effect of carrier particle shape on dry powder inhaler performance. Int J of pharm 2011; 421(1):12-23.

[19] Kaialy W, Nokhodchi A. The use of freeze-dried mannitol to enhance the in vitro aerosolization behaviour of budesonide from the Aerolizer®. Powder Technol 2016; 288: 291-302.

[20] Henninger, SK, Schicktanz M., Hugenell PPC. Sievers H, Henning HM. Evaluation of methanol adsorption on activated carbon for thermally driven chillers part I: Thermophysical characterisation. Int J Refrig 2012; 35(3): 543 -553.

[21] Krause U. Fires in Silos: Hazards, Prevention, and Fire Fighting. Wiley Publisher, VCH, (2009).

[22] Kaialy W., Alhalaweh A, Velaga SP, Nokhodchi, A. Influence of lactose carrier particle size on the aerosol performance of budesonide from a dry powder inhaler. Powder Technol 2012; 227:74-85.

[23] Healy AM. Particle Size Analysis. 2010, http://www.tcd.ie/cma/misc/particle.ppt

[24] Meunier F. Solid sorption: an alternative to CFCs .Heat Recovery Systems & CHP 1993;13(4):289-295.

[25] Sahoo PK, John M, Newalkar BL, Choudhary NV, Ayappa KG. Filling Characteristics for an Activated Carbon Based Adsorbed Natural Gas Storage System. *Ind Eng Chem* Res 2011; 50(23): 13000–13011.

[26] Fujioka K, Suzuki H. Thermophysical properties and reaction rate of composite reactant of calcium chloride and expanded graphite. Appl Therm Eng 2013; 50(2): 1627-1632.

[27] Wang LW, Tamainot-Telto, Z, Thrope R, Critoph RE, Metcalf SJ. Study of thermal conductivity permeability and adsorption performance of solidified composite activated carbon adsorbent for refrigeration. Renewable Energy 2011; **36**(8): 2062-2066.

[28] Hongyu H., Zhaohong H, Haoran Y, Noriyuki K, Dandan Z, Mitsuhiro K, Huafang G. Effect of Adsorbent Diameter on the Performance of Adsorption Refrigeration. Chinese J Chem Eng 2014; 22(5): 602-606.

[29] Zhao YJ, Wang LW, Wan RZ, Ma KQ, Jiang L. Study on consolidated activated carbon: Choice of optimal adsorbent for refrigeration application. Int J Heat Mass Transfer 2013; 67: 867–876.

[30] Critoph RE. Evaluation of alternative refrigerant-adsorbent pairs for refrigeration cycles. Appl Therm Eng 1996; 16(11): 891-900.

[31] Tamainot-Telto Z, Metcalf SJ, Critoph RE. Novel compact sorption generators for car air conditioning. Int J Refrig 2009; 32(4): 727-733.

[32] Bartell FE, Bower, JE Adsorption of vapors by silica gels of different structures. 1952. DOI: 10.1016/0095-8522(52)90022-6.

[33] Van Campen L, Amidon G.L, Zografi G. 1993. Moisture sorption kinetics for water-soluble substances. I. Theoritical considerations of heat transport control. J. Pharm. Sci. 72: 1381-1388.

[34] Çağlar A. Design and experimental testing of an adsorbent bed for a thermal wave adsorption cooling cycle. (Unpublished doctoral dissertation). *Middle East Technical University,* Ankara, 2012.

[35] Wang K, Wu JY, Wang RZ, Wang LW. Composite adsorbent of $CaCl_2$and expanded graphite for adsorption ice maker on fishing boats. Int J Refrig 2006 ; 29(2): 199–210.

[36] Dawoud, B, Sohel MI, Freni A, Vastac S, Restuccia G. On the effective thermal conductivity of wetted zeolite under the working conditions of an adsorption chiller. Appl Therm Eng 2011; 31(14-15): 2241-2246.

[37] Freni A, Tokarev MM, Restuccia G, Okunev, AG, Aristov YI. Thermal conductivity of selective water sorbents under the working conditions of a sorption chiller. Appl Therm Eng 2002; 22(14): 1631–1642.

[38] Gurgel JM, Oliveira PA, Ailson, S, Oliveira LG, Tavares F.R.M. Experimental results for thermal conductivity of adsorbed natural gas on activated carbon. 17th European conference on thermophysical properties, 2005.

[39] Jiang, L, Wang LW, Wang RZ. Investigation on thermal conductive consolidated composite $CaCl_2$ for adsorption refrigeration. Int JTherm Sci 2014; 81: 68-75.

[40] Zhao, YJ, Wang RZ, Wang LW, Yu N. Development of highly conductive KNO3/NaNO3 composite for TES (thermal energy storage). Energy 2014; **70**: 272-27.

[41] Hu P, Juan-Juan Y, Ze-Shao C. Analysis for composite zeolite/foam aluminum–water mass recovery adsorption refrigeration system driven by engine exhaust heat. Energy Convers Manage 2009; 50(2): 255–261.

[42] Ismail AB, Li A, Thu K, Ng KC, Chun W. Pressurized adsorption cooling cycles driven by solar/waste heat. Appl Therm Eng 2014; 67: 106-113.

[43] Attalla M, Sadek S. Experimental Investigation of Granular Activated Carbon/R-134a Pair for Adsorption Cooling System Applications. J Power Energy Eng, 2014;2:11-20

[44] Miyazaki T., El-Sharkawy, II, Saha, BB, Koyama S. Optimized Performance of One-Bed Adsorption Cooling System. International Refrigeration and Air Conditioning Conference, (2014).

[45] Habib K, Saha B. performance evaluation of solar driven activated carbon fiber-ethanol based adsorption cooling system in Malaysia, *Asian Journal of Scientific Research* 2013; ***6****:*146-156.

[46] Chekirou W, Boukheit N, Karaali, A. Optimal Design Study of Tubular Adsorber for Solid Adsorption Solar Cooling Machine Working with Activated Carbon–Methanol Pair. *16èmes Journées Internationales de Thermique (JITH 2013)*

[47] Rowe KC. Numerical analysis of multi-bed activated carbon/methanol adsorption refrigeration system with allowance for dynamic pressure variation. 3rd IIR Conference on Cold Chain and Sustainability, London, 2014.

[48] Jerai F, Miyazaki T, Saha B, Koyama S. Overview of adsorption cooling system based on activated carbon –Alcohol Pair. Joint Journal of Novel carbon resources Sciences & green Asia Stratgy 2015; 30-40.

[49] Hassan HZ. Energy Analysis and Performance Evaluation of the Adsorption Refrigeration System. ISRN Mechanical Engineering. http://dx.doi.org/10.1155/2013/704340.

[50] He ZH, Hu HY, Deng LS, Yuan HR, Kobayashi N , Kubota M, Huhetaoli, Zhao DD. Development of novel type of two-stage adsorption chiller with different adsorbents.

The 6th International Conference on Applied Energy – ICAE2014, *Energy Procedia*, 2014; 61: 1996 – 1999.

[51] Shmroukh, AN, Ali AHH , Abel-Rahman AK. Adsorption Refrigeration Working Pairs: the state-of-the-art in the application. Int J Chemical, Mater Sci Eng 2013;7 (11b) : 793- 805.

[52] Shmroukh, AN, Ali AHH, Abel-Rahman AK , Ookwara S. Experimental Investigation on Adsorption Capacity of a Variety of Activated Carbon/Refrigerant Pairs. Int J Eng Res Appl 2015; **5**(4) P-6: 66-76.

[53] Umair M, Akisawa A, Ueda Y. Simulation Study of Continuous Solar Adsorption Refrigeration System Driven by Compound Parabolic Concentrator. The Open Renewable Energy J 2014; **7**:1-12.

[54] Habib K, Majid MA, Sulaiman SA. Study on two stage activated carbon/HFC-134a based adsorption chiller. 4th International Conference on Energy and Environment 2013; 16: 012084.

[55] Ramji HR, Leo SL, Tan IAW, Abdullah MO. Comparative study of three different adsorbent-adsorbate working pairs for a waste heat driven adsorption air conditioning system based on simulation. IJRRAS 2014; 18(2): 109-121.

[56] Habib K, Saha BB, Koyama S. Study of various adsorbent-refrigerant pairs for the application of solar driven adsorption cooling in tropical climates. Appl Therm Eng. 2014; 72: 266-274.

[57] Jribi S, Saha BB, Koyama S, Bentaher H. Modeling and simulation of an activated carbon–CO2 four bed based adsorption cooling system. Energy Convers Manage 2014; 78: 985–991.

[58] Jribi S., Saha B.B., Koyama, S., Chakraborty, A., Ng, K.C. Study on activated carbon/HFO-1234ze(E) based adsorption cooling cycle. Appl Therm Eng 2013; 50: 1570-1575.

[59] Uddin K, El-Sharkawy II, Miyazaki T, Saha BB, Koyama S, Kil HS, Miyawaki J, Yoon SH. Adsorption characteristics of ethanol onto functional activated carbons with controlled oxygen content. Appl Therm Eng 2014; 72: 211-218.

[60] El-Sharkawy II, Uddin K, Miyazaki T, Saha BB, Koyama S, Miyawaki J, Yoon SH. Adsorption of ethanol onto parent and surface treated activated carbon powders. Int J Heat Mass Transfer 2014; 73: 445–455.

[61] Askalany AA, Saha, BB, Ismail IM. Adsorption isotherms and kinetics of HFC410A onto activated carbons. App Therm Eng 2014; 72: 237-243.

[62] Askalany AA, Saha BB. Experimental and theoretical study of adsorption kinetics of Difluoromethane onto activated carbons. Int J Refrig. 2015 4(9) 160-1 68.

[63] Anyanwu E , Ogueke N. Thermodynamic design procedure for solid adsorption solar refrigerator. Renewable Energy 2005; 30:81–96.

[64] Wang LW, Wang RZ, Oliveira RG. A review on adsorption working pairs for refrigeration. Renewable Sustainable Energy Rev 2009a, 13, 518–534.

[65] Mugnier D, Goetz V. Energy storage comparison of sorption systems for cooling and refrigeration. Sol Energy 2001 ;(71): 47–55.

[66] San, JY, Lin, WM. Comparison among three adsorption pairs for using as the working substances in a multi-bed adsorption heat pump. Appl Therm Eng 2008, 28, 988–997.

[67] Jribi S, El-Sharkawy I I, Koyama S, Saha BB. Study on activated carbon-co2 pair: adsorption characteristics and cycle performance. International Symposium on Next-generation Air Conditioning and Refrigeration Technology, 2010b.

[68] Saha, B.B., Habib, K., El-Sharkawy, I.I. & Koyama, S. Adsorption characteristics and heat of adsorption measurements of R-134a on activated carbon. Int J Refrig 2009; 32(7): 1563–1569.

[69] Jribi S, Chakraborty A, El-Sharkawy I, Saha BB, Koyama S. Thermodynamic Analysis of Activated Carbon CO2 based Adsorption Cooling Cycles. Int J Eng Nat Sci 2009; 3(3): 142-145.

[70] Jribi S, Koyama S, Saha BB. Performance Investigation of a Novel CO2 Compression-Adsorption Based Hybrid Cooling Cycle. Engineering Sciences Reports, Kyushu University 2010a; 32(3): 12-18.

[71] Anupam K, Chatterjee A, Halder GN, Sarkar SC. Experimental investigation of a single-bed pressure swing adsorption refrigeration system towards replacement of halogenated refrigerants. Chem Eng J 2011a; 171(2); 541–548.

[72] Loh WS, El-Sharkawy, II, Ng KC, Saha, BB. Adsorption cooling cycles for alternative adsorbent/adsorbate pairs working at partial vacuum and pressurized conditions. 2009

[73] Saha B, Chakraborty A, Koyama S, Aristov YI. A new generation cooling device employing $cacl_2$-in-silica gel-water system. Int J heat and Mass Transfer 2009; 52(1-2): 516-524.

[74] Loh W, Shah B, Chakraborty A, NG K, Chun W. Performance analysis of waste heat driven pressurized adsorption chiller. J Therm Sci Tech 2010; 5 (2):252-265

[75] Jiayou Q. Characterization of silica gel-water vapor adsorption and its measuring facility. (Unpublished master dissertation). National University of Singapore, Singapore, 2003.

[76] Kumar M. Adsorption of methane on activated carbon by volumetric method. (Unpublished master dissertation). National Institute Of Technology, Rourkela, 2011.

[77] Cui Q, Tao G, Chen H, Guo X, Yao H. Environmentally benign working pairs for adsorption refrigeration. Energy 2005; 30(2-4): 261–271.

[78] Ivanova EP, Kostova MA, Koumanova BK. Kinetics of water and alcohol vapors adsorption on natural zeolite. Asia-Pacific J Chem Eng 2010; 5(6): 869–881.

[79] El-Sharkawy, II, Kuwahara K, Saha BB, Koyama S, KC Ng. Experimental investigation of activated carbon fibers/ethanol pairs for adsorption cooling system application. Appl Therm Eng 2006; 26(8-9): 859–865.

[80] Elsayed A, AL-Dadah RK, Mahmoud S, Kaialy W. Investigation of activated carbon /Ethanol for low temperature adsorption cooling. Int J Green Energy 2014, Manuscript ID IJGE: 0320.

[81] Ming HJ. Adsorption evaporative emission control system for vehicles. (Unpublished doctoral dissertation). *National University of Singapore*, Singapore, 2009.

[82] Sapienza A, Santamaria S, Frazzica A, Freni A, Aristov YI. Dynamic study of adsorbers by a new gravimetric version of the Large Temperature Jump method. Appl Energy 2014; 113: 1244–1251.

[83] Ahamat, MA, Tierney MJ. Calorimetric assessment of adsorbents bonded to metal surfaces: Application to type A silica gel bonded to aluminium. Appl Therm Eng 2012; 40: 258-266.

[84] Füldner G, L Schnable. Non-isothermal kinetics of water adsorption in compact adsorbent layers on a metal support. Comsol conference proceeding, Hannover. 2008, http://www.comsol.com/papers/5118/

[85] Demir H, Mobedi M, Ulku S. Microcalorimetric investigation of water vapor adsorption on silica gel. J Therm Anal Calorim 2011; 105:375-382.

[86] Wang LW, Wang RZ, Lu ZS, Chen CJ, Wang K, Wu JY. The performance of two adsorption ice making test units using activated carbon and a carbon composite as adsorbents. Carbon 2006; 44(13): 2671–2680.

[87] Zhong Y, Critoph RE, Thorpe RN, Tamainot-Telto Z. Dynamics of BaCl2–NH3 adsorption pair. Appl Therm Eng 2009; 29(5-6): 1180–1186.

[88] Riffat SB, Williams MD, Stuart C. Adsorption heat pump using HFC refrigerants. Int J Energy Res 1997; 21(6): 481-494.

[89] Ulku S. Adsorption heat pumps. Heat Recovery Systems 1986; 6(4): 277-284

[90] Daou K., Wang RZ, Yang, GZ, Xia ZZ. Theoretical comparison of the refrigerating performances of a $CaCl_2$ impregnated composite adsorbent to those of the host silica gel. Int J Therm Sci 2008;47(1):68–75

[91] Habib K, Saha, BB, Rahman KA, Chakraborty A, Koyama S, Ng KC. Experimental study on adsorption kinetics of activated carbon/R134a and activated carbon/R507A pairs. Int J Refrig 2010; 33(4): 706 – 713.

[92] Aristov Y I , Dawoud B, Glaznev IS, Elyas A. A new methodology of studying the dynamics of water sorption/desorption under real operating conditions of adsorption heat pumps: Experiment. Int J Heat Mass Transfer 2008; 51(19–20): 4966–4972.

[93] Chan KC, Chao CYH, Sze-To GN, Hui KS. Performance predictions for a new zeolite 13X/$CaCl_2$ composite adsorbent for adsorption cooling systems. Int J Heat Mass Transfer 2012,; **55**(11-12): 3214–3224.

[94] Tso CY, Chao CYH, Fu SC. Performance analysis of a waste heat driven activated carbon based composite adsorbent – Water adsorption chiller using simulation model. Int J Heat Mass Transfer 2012a; 55(25-26): 7596–7610.

[95] Chua HT, Ng KC, Malek A. Modeling the performance of two bed, silica gel– water adsorption chiller. Int J Refrig 1999; 22: 194–204.

[96] Boelman EC, Saha BB, Kashiwagi T. Parametric study of a silica gel–water adsorption refrigeration cycle – the influence of thermal capacitance and heat exchanger UA-values on cooling capacity, power density and COP. ASHRAE Trans 1997; 103(1): 139–48.

[97] Wang X, Chua HT. Two bed silica gel–water adsorption chillers: an effectual lumped parameter model. Int J Refrig 2007; 30(8):1417–26.

[98] Wu WD, Zhang H, Sun DW. Mathematical simulation and experimental study of a modified zeolite 13X–water adsorption refrigeration module. Appl Therm Eng 2009; 29(4): 645–651.

[99] Saha BB, Boelman EC, Kashiwa T. Computer simulation of a silica gel–water adsorption refrigeration cycle – the influence of operating conditions on cooling output and COP. ASHRAE Trans 1995; 101: 348–57.

[100] Miyazaki, T., & Akisawa, A. The influence of heat exchanger on the optimum cycle time of adsorption chiller. Appl Therm Eng 2009; 29: 2708-2717.

[101] Schicktanz M , Núñez T. Modelling of an adsorption chiller for dynamic system simulation. Int J Refrig 2009; 32: 588–95.

[102] Vasta S, Frazzica A, Maggio G. Simulation of a small size solar assisted adsorption air conditioning system for residential application. In: Proceedings of the heat powered cycles conference. TU, Berlin, 2009.

[103] Maggio G, Gordeeva LG, Freni A, Aristov YuI, Santori G, Polonara F, Restuccia G . Simulation of a solid sorption ice-maker based on the novel composite sorbent ‘‘lithium chloride in silica gel pores” . Appl Therm Eng 2009; 29(8-9): 1714–1720.

[104] Wang X, Chua HT. A comparative evaluation of two different heat-recovery schemes as applied to a two-bed adsorption chiller. Int J Heat Mass Transfer 2007; 50 (3-4):433–43.

[105] Freni A, Maggio G, Cipitì F, Aristov I. Simulation of water sorption dynamics in adsorption chillers: One, two and four layers of loose silica grains. Appl Therm Eng 2012;44: 69-77.

[106] Mahdavikhah M, Niazmand H. Effects of plate finned heat exchanger parameters on the adsorption chiller performance. Appl Therm Eng 2013; 50: 939-949.

[107] Elsayed A, Mahmoud S, Al-Dadah R, Bowen J, Kaialy W. Experimental and numerical investigation of the effect of pellet size on the adsorption characteristics of activated carbon/ethanol. Energy Procedia 2014; (61): 2327 – 2330

[108] Aristov YI. Adsorptive transformation of heat: Principles of construction of adsorbents database. Appl Therm Eng 2011; 42: 18-24.

[109] Do DD. Adsorption Analysis: Equilibria and Kinetics. Series on chemical Engineering, Imperial College Press, London, (1998).

[110] Saha BB, Koyama S, El-Sharkawy II, Habib K, Srinivasan K, Dutta P. Evaluation of Adsorption Parameters and Heats of Adsorption through Desorption Measurements. J. Chem. Eng. Data 2007; 52: 2419-2424.

[111] Tiansuwan J, Hirunlabh J, Kiatsiriroat T. Mathematical Model of an Activated Carbon-Ethanol Refrigerator. Thammast Int J Sc Tech 1998; 3(l).

[112] Follin S, Goetz V, Guillot A. Influence of microporous characteristics of activated carbons on the performance of an adsorption cycle for refrigeration. Ind Eng Chem Res 1996; 35(8): 2632-2639.

[113] Cevallos O. Adsorption characteristics of water and silica gel system for desalination cycle. King Abdullah University of Science and Technology, Thuwal, Kingdom of Saudi Arabia. 2012.

[114] El-Sharkawy II, Saha BB, Shigeru K, Kim CN. A study on the kinetics of ethanol-activated carbon fiber: Theory and experiments. Int J Heat Mass Transfer 2006; (17-18): 3104–3110.

[115] Hong, S.W., Kwon O.K, Chung J.D. Application of an embossed plate heat exchanger to adsorption chiller. International Journal of refrigeration 2016, 65: 142-53.

[116] Niazmand H, Talebian H, Mahdavikhah M. Effects of particle diameter on performance improvement of adsorption systems. Applied thermal engineering 2013, 59:243-252.

[117] Hong S, Ahn S, Kwon O, Chung J. Validity of intra-particle models of mass transfer kinetics in the analysis of a fin-tube type adsorption bed. J. Mech. Sci. Technol. 2014, 28(5): 1985-1993.

[118] Rahman KA. Experimental and theoretical studies on adsorbed natural gas storage system using activated carbons. PhD thesis, National University of Singapore 2011.

Figures

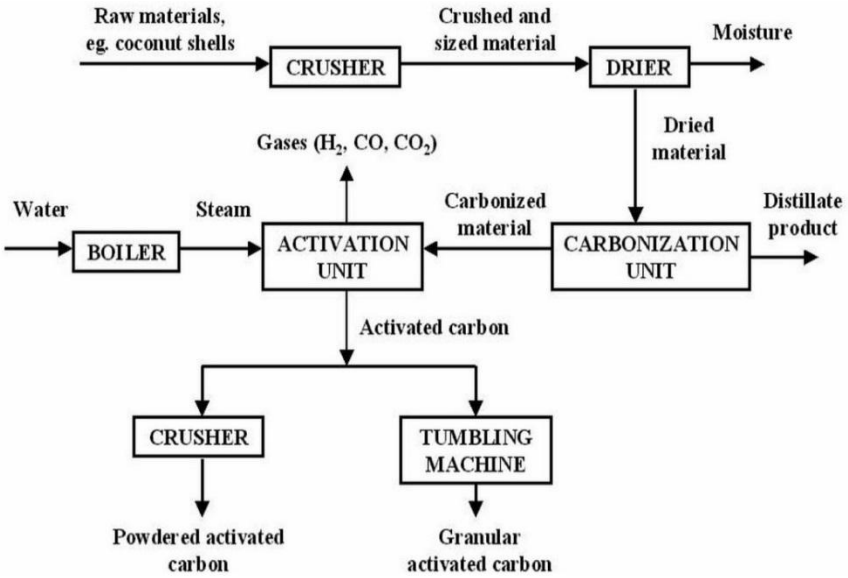

Fig. 1. Flow diagram of activated carbon production **[9]**

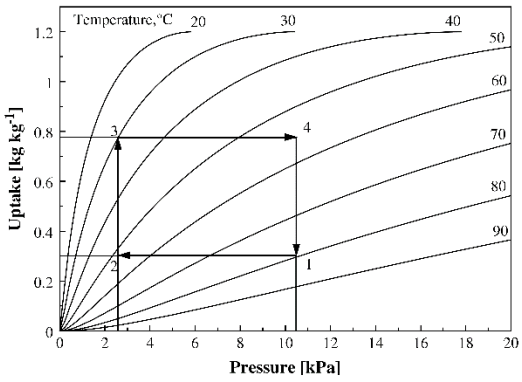

Maxsorb III-ethanol pair **[12]**

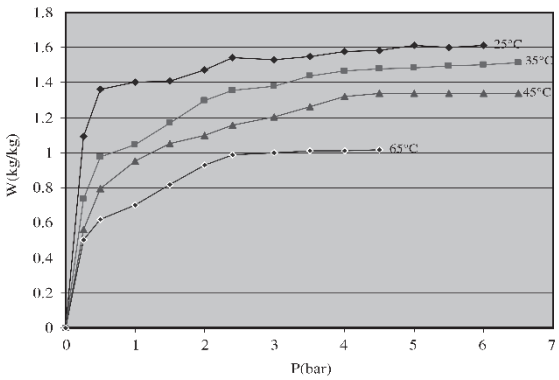

Granular activated carbon/HFC134a pair **[13]**

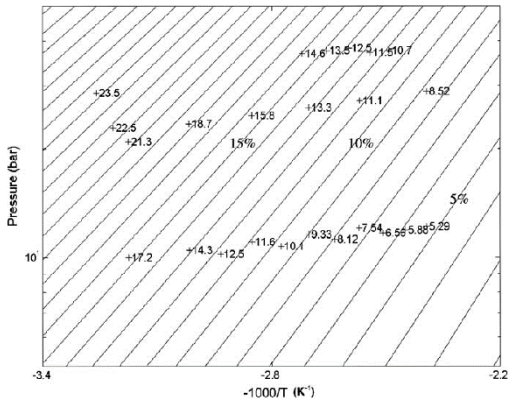

Clayperon diagram for AC/Co_2 **[14]**

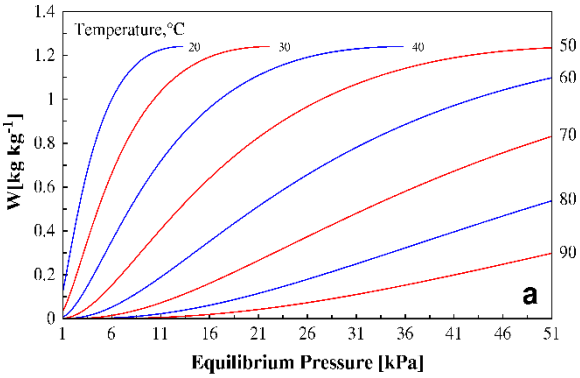

Maxsorb III/methanol **[15]**

Fig. 2. Uptake of different carbon based pairs

(a) Sieving analysis

(b) Photo sedimentation technique

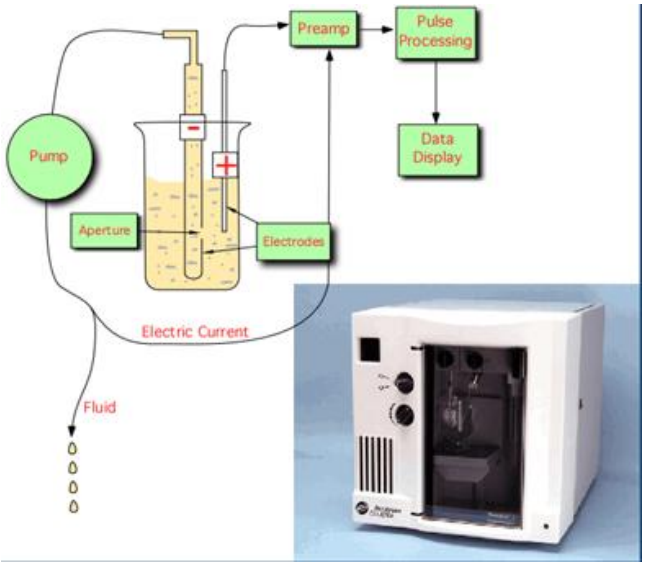

(c) Electrical sensing zone method

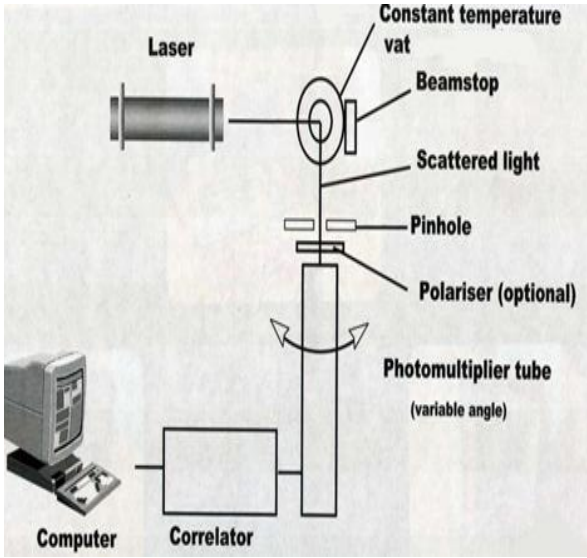

(d) Photon Correlation Spectroscopy

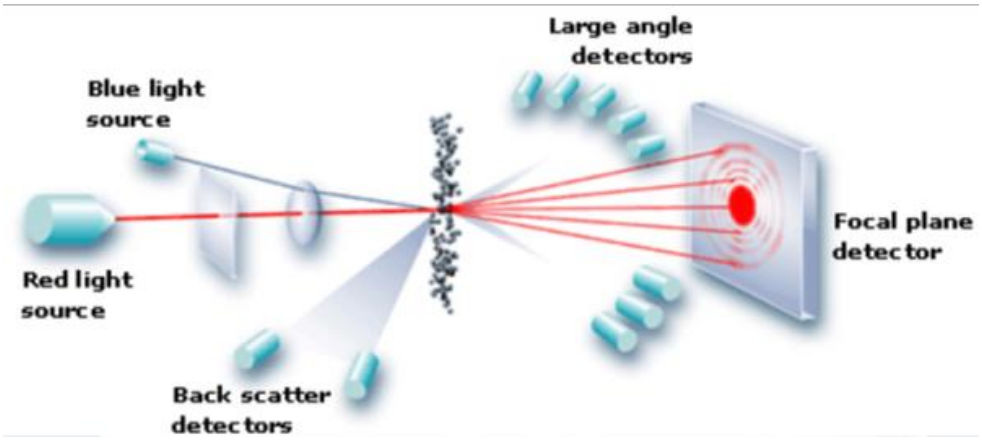

(e) Laser diffraction

Fig. 3: Different techniques for measuring powder particle sizes. **[23]**

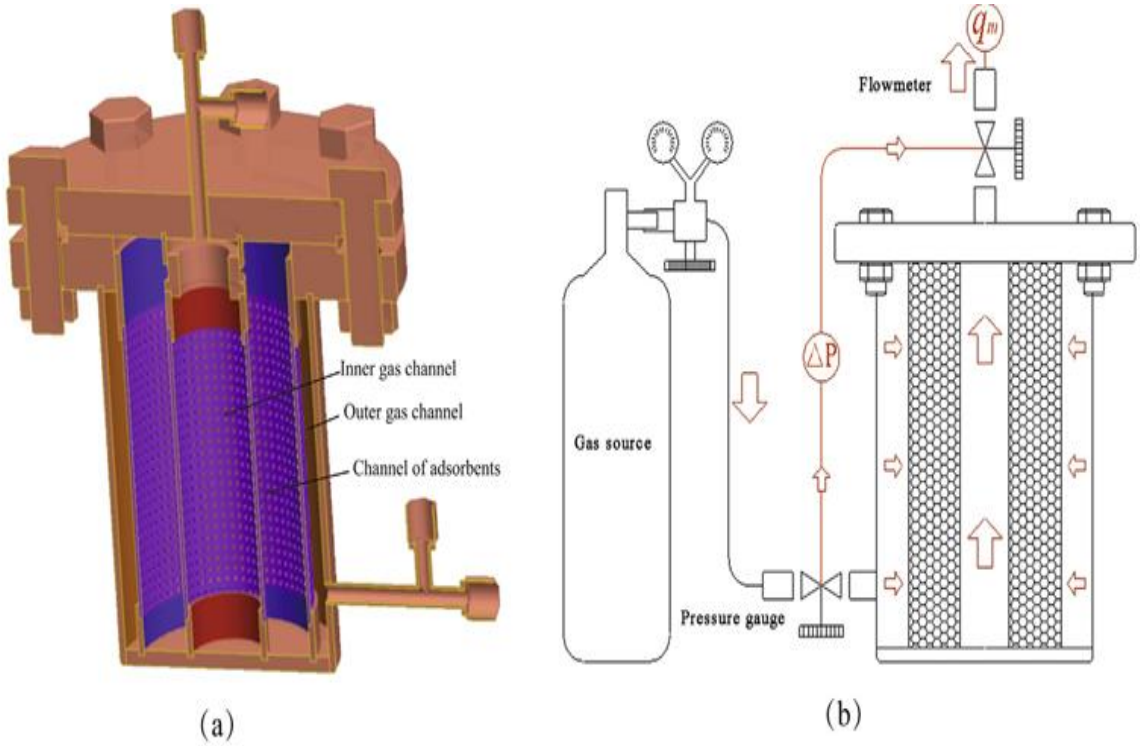

Fig. 4. Permeability test facility **[29]**

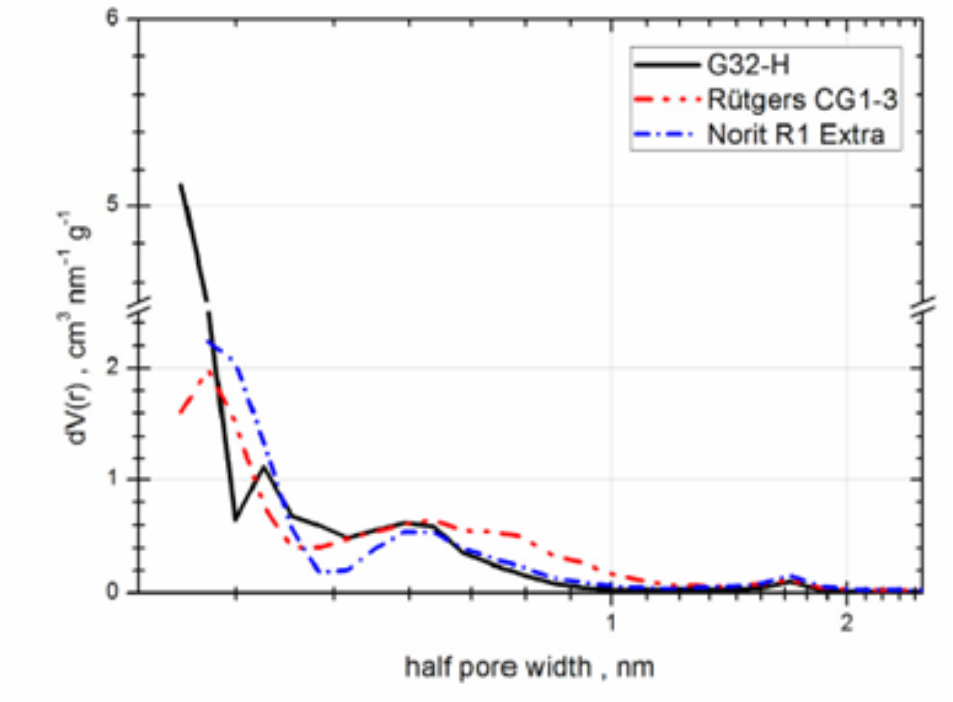

Fig. 5. Methanol pore size distribution function for different carbon samples **[20]**

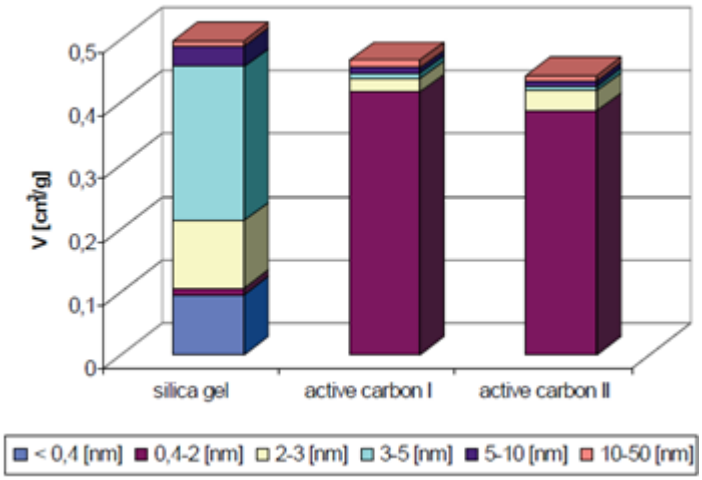

Fig. 6. Comparison of the pore volume for three different sorbents **[17]**

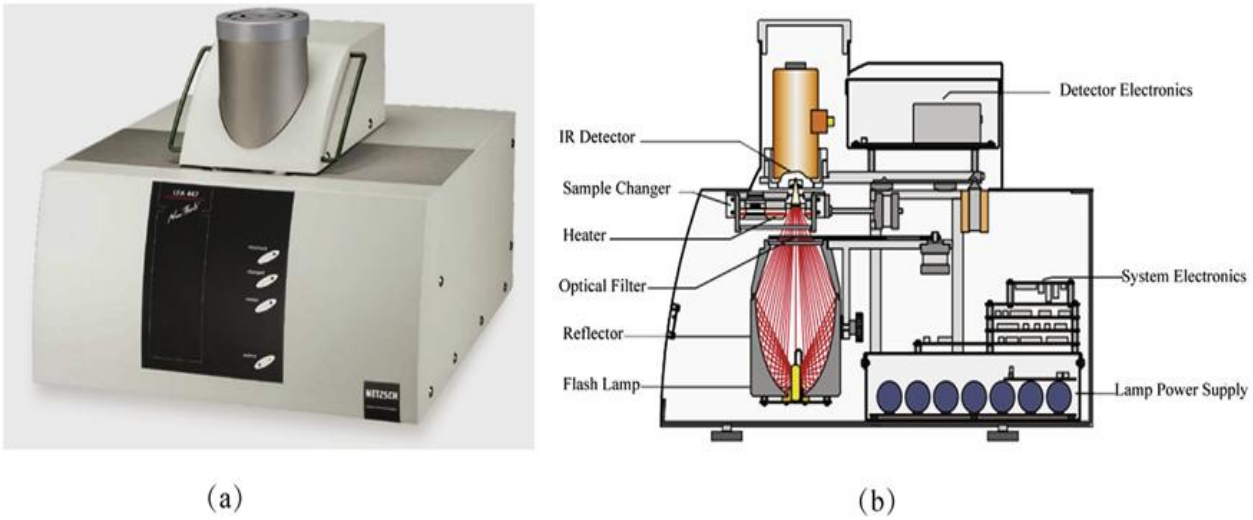

Fig. 7. Laser beam thermal conductivity measurement technique **[29]**

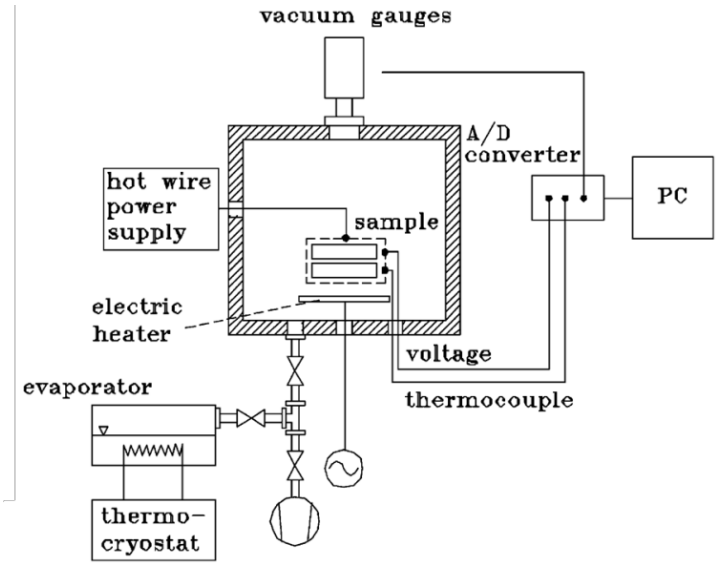

Fig. 8. Hot wire thermal conductivity measurement technique **[37]**

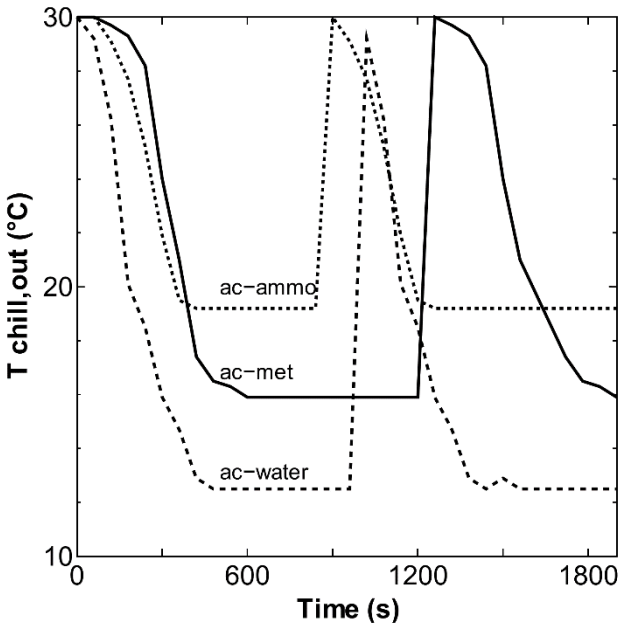

Fig. 9: Temperature distribution of chilled fluid in evaporator during cycle time for different refrigerants based on activated carbon. **[55]**

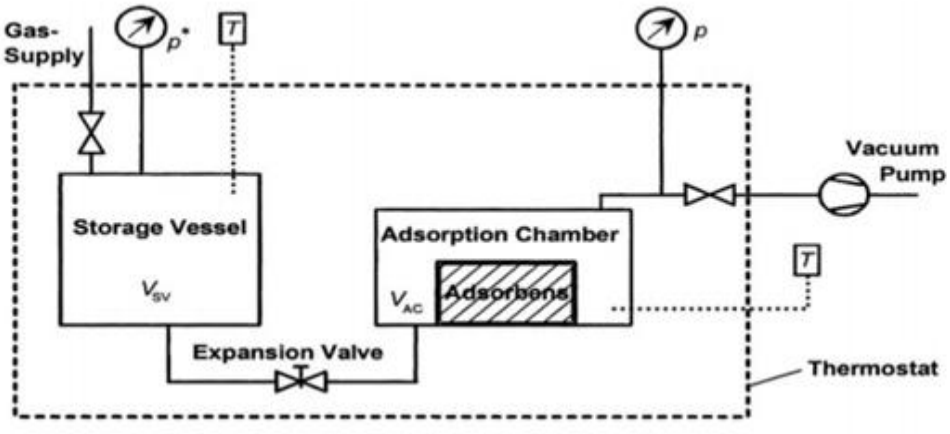

Fig. 10. Volumetric technique for measuring adsorption isotherms **[76]**

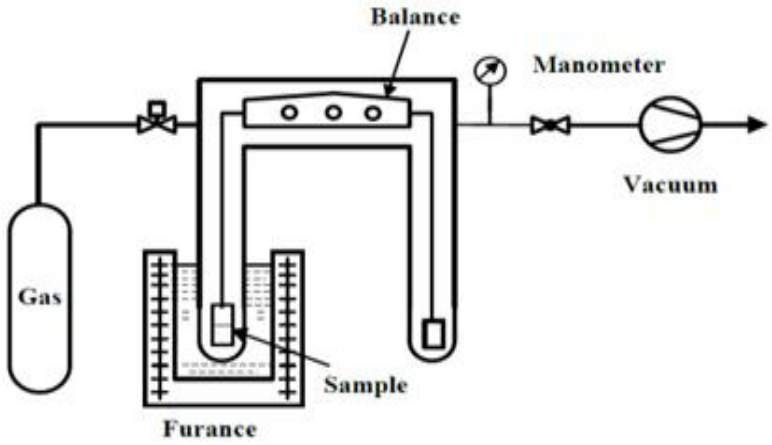

Fig. 11. Gravimetric concept of isotherm measurements **[76]**

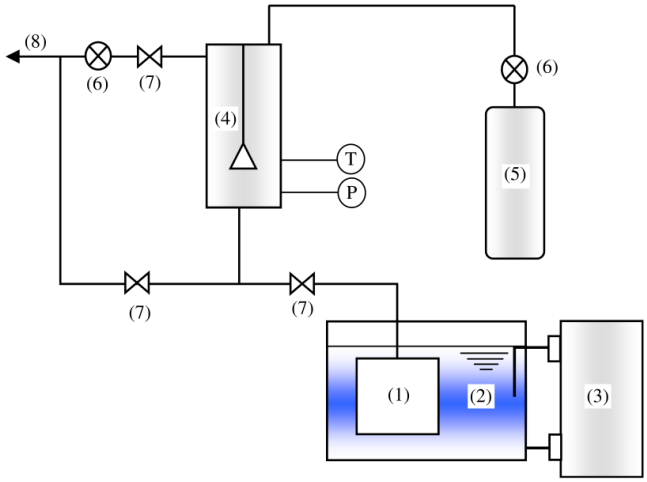

Fig. 12. TGA test facility **[12].** (1)Evaporator; (2)Constant temperature water bath; (3) Water circulator; (4)TGA reacting chamber; (5)Helium cylinder; (6) Pressure regulator; (7) Valve; (8) To the vacuum pump.

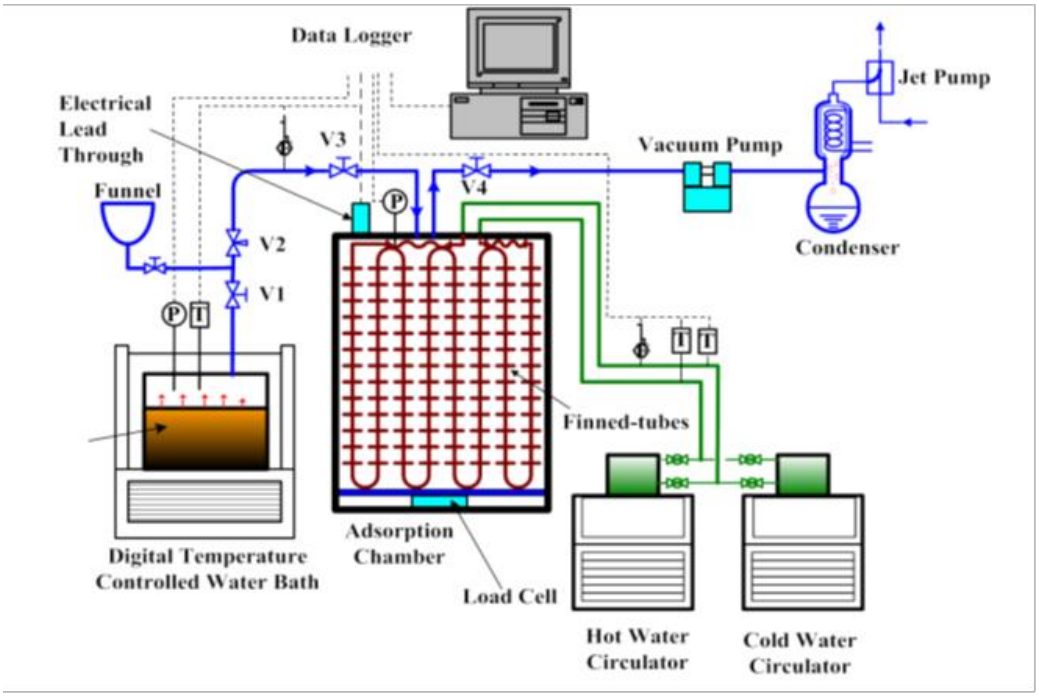

Fig. 13. Load cell sensor technique used by Ming **[81]**

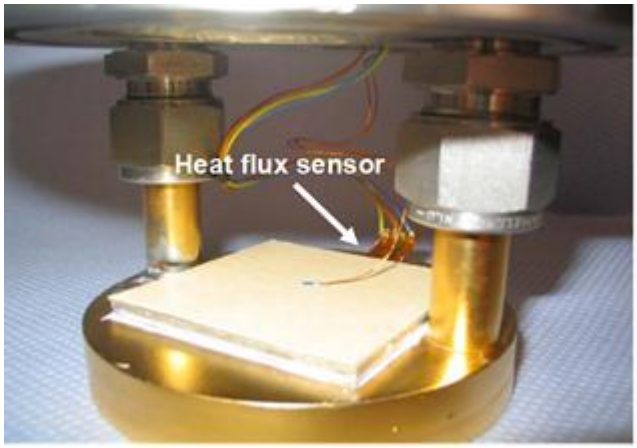

Fig. 14. Heat flux sensor technique used by Füldner and Schnabel **[84]**

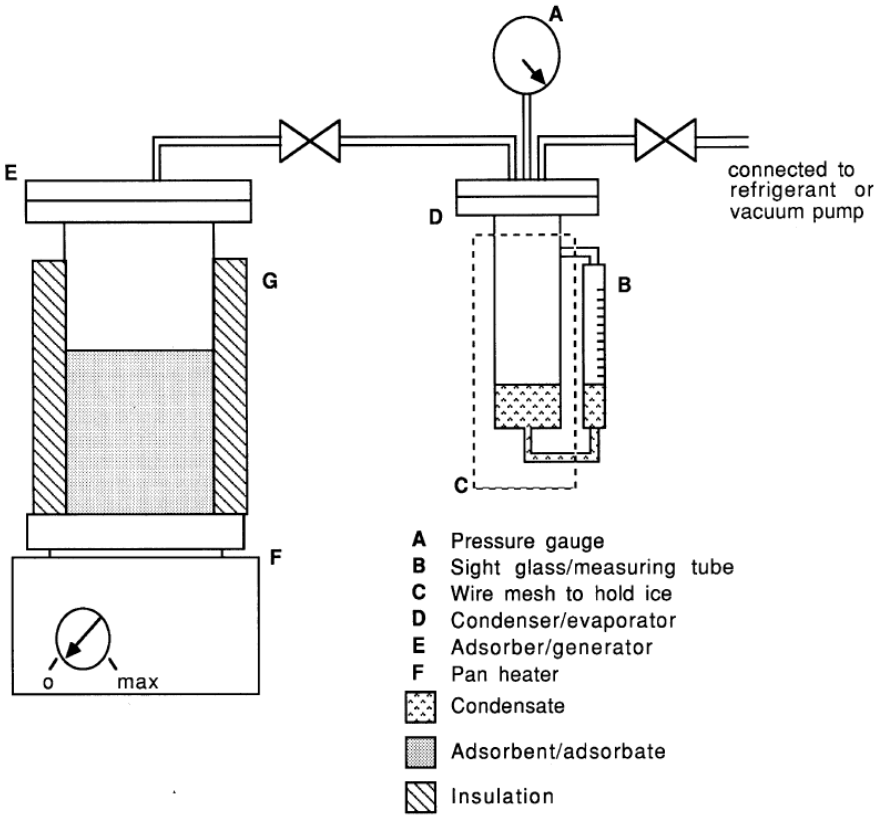

Fig. 15. Manual refrigerant liquid recording **[88]**

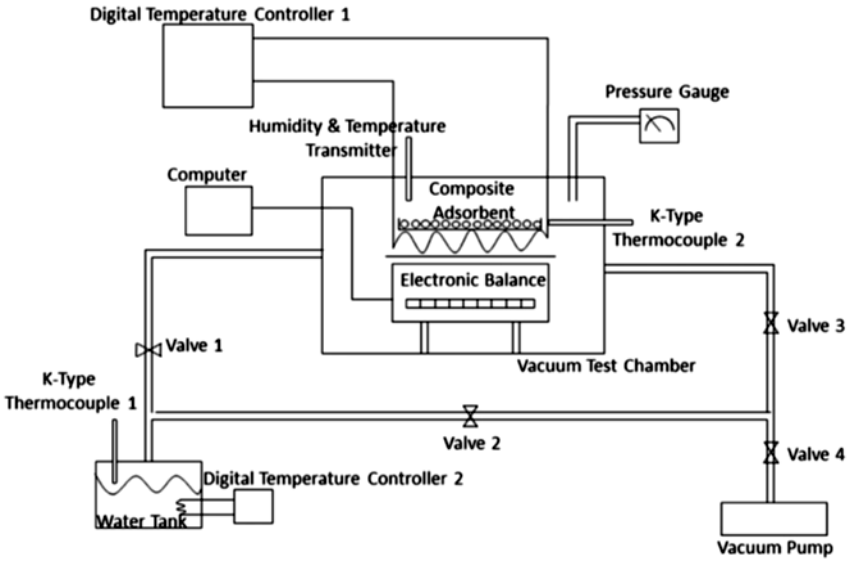

Fig. 16. Measurements by electronic balance by Tso et al. **[94]**

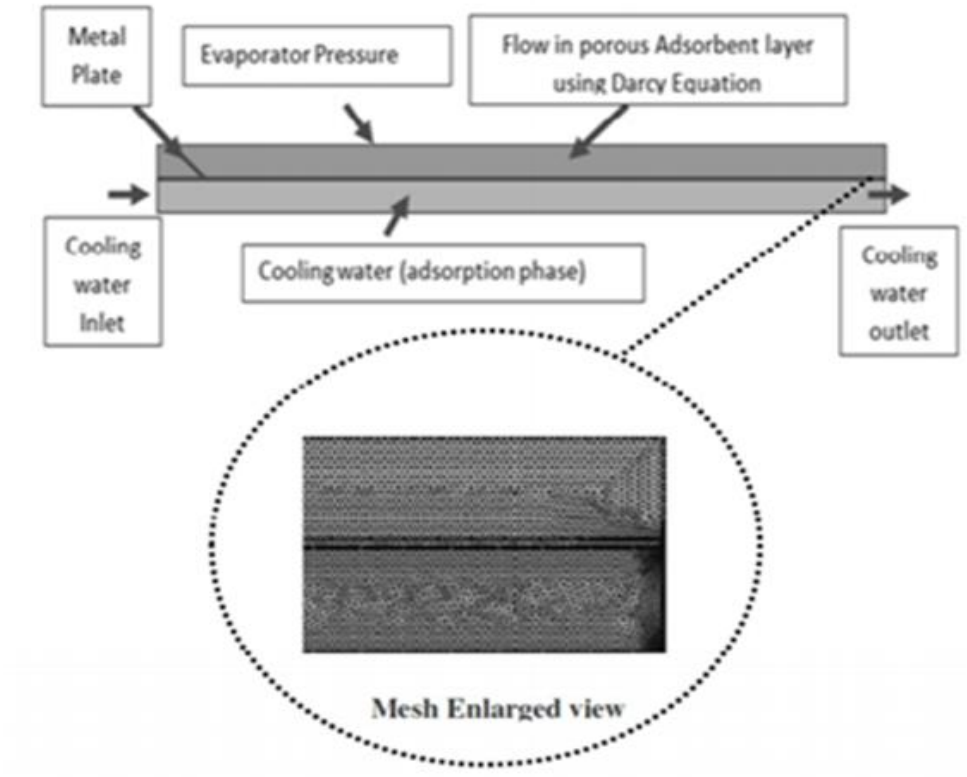

Fig. 17. Plate type adsorber configuration for the CFD modeling **[80]**

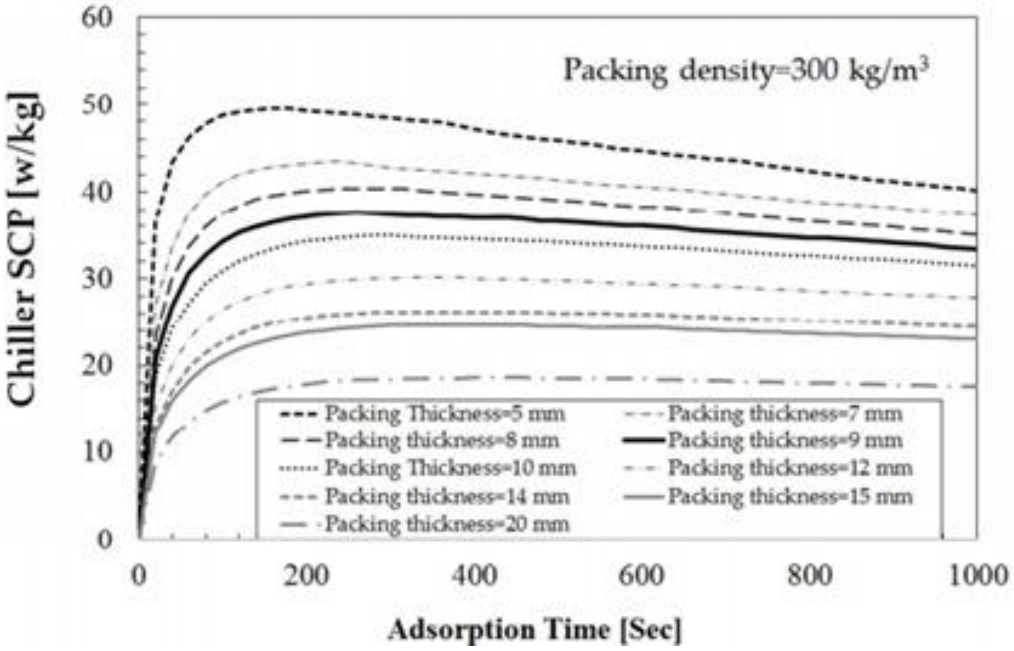

Fig. 18. Chiller SCP at various adsorbent thicknesses **[80]**

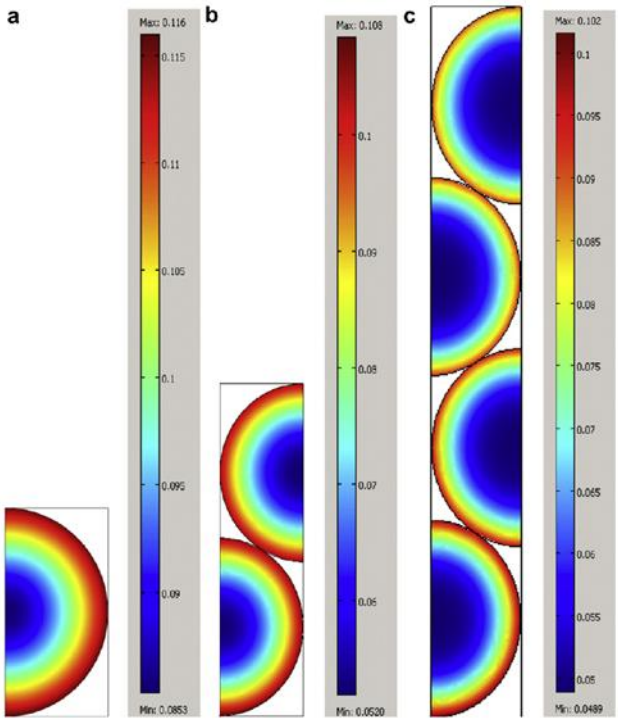

Fig. 19. Water /silica gel uptake mapping for 20 s of simulation of adsorption process, calculated for a) one-grain, b) two-grain and c) four-grain configurations **[105]**

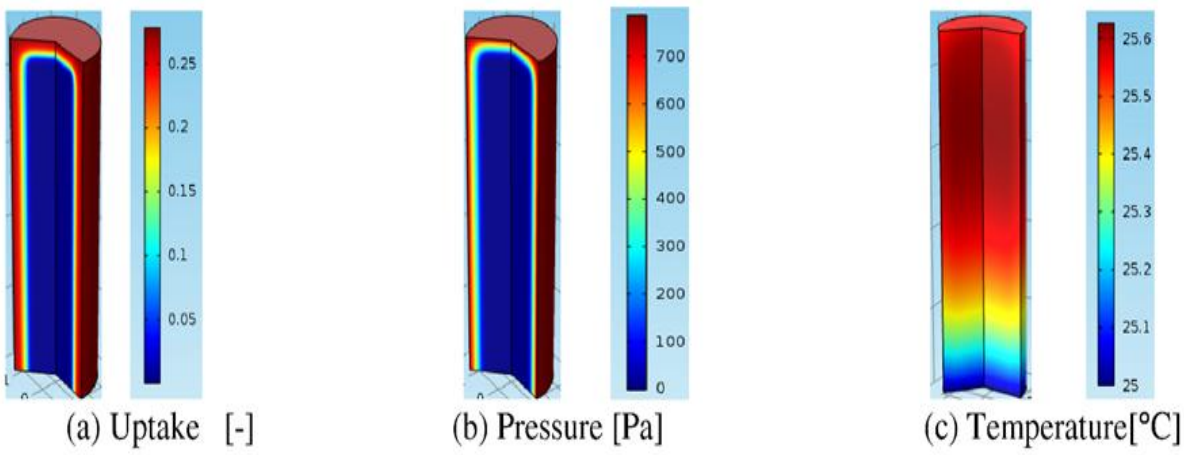

Fig. 20. Uptake, pressure, and temperature distribution in single adsorbent NX3/Ethanol pellet at 400 s **[107]**

Tables citations

Table 1. Techniques to determine the particle size.

Table 2. Physical characteristics of activated carbon samples.

Table 3. Refrigerants, working temperatures and Specific Cooling Power (SCP) for adsorption refrigeration systems using activated carbon adsorbent.

Table 4. Comparison of kinetic measurement techniques.

Table 5. Comparison of mathematical models.

Table 1. Techniques to determine the particle size.

Method	Advantages	Disadvantages
• Sieving Techniques	•Ease of operation •Wide size range •Inexpensive	• Reproducibility • Wear/damage during use or cleaning • Irregular (e.g. elongated) particles: overestimation of size distribution • Labour intensive
• Sedimentation Technique	•Equipment required can be relatively simple and inexpensive. •Can measure a wide range of sizes with accuracy and reproducibility	• Sedimentation analyses must be carried out at concentrations that are sufficiently low for interactive effects between particles to be negligible so that their terminal falling velocities can be taken as equal to those of isolated particles • Large particles create turbulence - thus are slowed and recorded undersize • Particle re-aggregation during extended measurements may occur. • Precise temperature control is necessary to suppress convection currents • The lower limit of particle size is set by the increasing importance of Brownian motion for progressively smaller particles • Particles have to be completely insoluble in the suspending liquid
• Electrical Sensing Zone Method	•True volume distribution •High resolution •Wide range of measurement: particle diameter from approx. 0.5-400µ	• Needs calibration • Medium must be an electrolyte • Low particle concentration • Errors with porous particles • Orifice blocking troublesome • Particles below minimum detectable size go unnoticed • Difficult with high density material
• Laser Diffraction	•Non-intrusive: uses a low power laser beam •Fast: typically <3 minutes to take a measurement and analyse it •Precise and wide range up to 64 size bands can be displayed covering a range of up to 100,000:1 in size. •Easy to use. •Absolute measurement - No calibration required (the instrument is based on fundamental physical properties).	• expensive • volume measurement - all other outputs are numerical transformations of this basic output form, assuming spherical particles • there must be a difference in refractive indices between particles and suspending medium • particle size recordings are influenced by particle shape, surface roughness and orientation
• Photon Correlation Spectroscopy	•Non-intrusive •Fast •Nanometre size rang	• Vibration and temperature fluctuations can interfere with analysis • Restricted to solid in liquid or liquid in liquid samples • Expensive • Need to know viscosity values

Table 2. Physical characteristics of AC samples **[20]**

Sample	Cp		Bulk density	True density	Calc. porosity ε form Hg intrusion
	T/°C	J g^{-1} K^{-1}	g cm^{-3}	g cm^{-3}	
G32-H	40	0.86	0.37 ± 0.04	2.174 ± 0.002	0.77
	80	0.95			
	120	1.05			
RUTGERS CG1-3	40	0.84	0.37 ± 0.04	2.139 ± 0.002	0.87
	80	0.95			
	120	1.05			
Norit R 1 Extra	40	0.88	0.42 ± 0.03	2.259 ± 0.007	0.84
	80	0.95			
	120	1.04			
Norit RX 3 Extra	40	0.83	0.37 ± 0.03	2.169 ± 0.001	0.75
	80	0.97			
	120	1.04			
CarboTech C40/1	40	0.78	0.38 ± 0.03	2.142 ± 0.001	0.82
	80	1.0			
	120	1.06			
Carbotech A35/1	40	0.86	0.33 ± 0.03	2.191 ± 0.002	0.88
	80	0.95			
	120	1.05			

Table 3. Refrigerants, working temperatures and Specific Cooling Power (SCP) for adsorption refrigeration systems using activated carbon adsorbent.

Author	Pair	Tevap [˚C]	Tcond/ Tads[˚C]	Tdes [˚C]	SCP [W/kg]
Ismail *et al*. (2014) **[42]**	R32 R507 R290 R134a	-5 to 20	30	85	
Attalla *et al*. (2014) **[43]**	Granular GAC/R134a pair (Characterization)		20-60	60 to 105	
Miyazaki *et al*.(2014) **[44]**	Chemically treated Maxsorb/Ethanol (characterization)	14	30	80	140
Habib and Saha (2013) **[45]**	AC fiber ACF-20/ethanol	14	30	85	12 [kW]
Chekirou *et al*. (2013) **[46]**	AC-35/Methanol (Solar cooling)				
Rowe *et al*. (2014) **[47]**	Ac/Methanol	5	30/25	90	327
Jerai *et al*. (2015) **[48]**	AC KOH-6/Ethanol				
Hassan (2013) **[49]**	AC/Methanol	-5	30	120	
He *et al*. (2014) **[50]**	Zeolite and AC combined cycle	15	30	50	200 [W/L]
Shmroukh *et al*. (2013, 2015) **[51, 52]**	R-134a,R-407c, R-507A In both powder and granular form			80	
Umair *et al*. (2014) **[53]**	Activated carbon fiber/Ethanol				80 [KJ/kg]
Habib *et al*. (2013) **[54]**	AC/R134a	14	30	70	8 kW
Ramji *et al*. (2014) **[55]**	AC/Water AC/Methanol AC/Ammonia			120	0.98[kW] 0.65[kW] 0.5[kW]
Habib *et al*. (2014) **[56]**	ACF/Ethanol AC/Methanol Silica gel/water	14	30	85	Less than 20 kW
Jribi *et al*. (2014) **[57]**	Co2/Maxsorb	15	27 to 37	50 to 95	1.7 kW
Jribi *et al*. (2013) **[58]**	AC/HFO1234ze(E)	15	30	85	2 kW
Uddin *et al*. (2014) **[59]** El-Sharkawy *et al*. (2014) **[60]**	Maxsorb III KOH-H2 Maxsorb III H2 treated Maxsorb III	-14 °C to77 °C		20 °C to 80 °C	
Askalany *et al*. (2014) **[61]**	Maxsorb III /R410A ACFiber A-20/R410A			10 °C to 50°C	
Askalany and Saha (2015) **[62]**	Maxsorb III /R32 ACFiber A-20/R32			25 °C to 65°C	

Table 4. Comparison of kinetic measurement techniques.

Measurement technique	Concept	Sensors required	Principals	Direct Data logging	Quantity of adsorbent
Microbalance	Gravimetric	Sensitive Mass scale	Direct mass measurements	√	Small quantities (few milligrams)
Adsorption heat measurements	Calorimetric	Heat flux sensor	Adsorption heat converted to uptake	√	Both large and small quantities
		Thermoelectric	Adsorption heat converted to uptake	√	Both large and small quantities
Load cell	Gravimetric	Load cell sensor	Voltage output signal converted to uptake	√	Large quantities
Liquid column	volumetric	Digital microscope	Observed liquid column converted to uptake	Manual recording of uptake	Large quantities
		Magnetostrictive Liquid level sensor	Liquid column converted to uptake	√	Large quantities
		transparent glass vessel	Observed liquid column converted to uptake	Manual recording of uptake	Large quantities
		Pressure differential sensor	Pressure difference converted to uptake	√	Large quantities
constant volume variable pressure method	Volumetric	Pressure and temperature sensors	Equation of state utilized to track the adsorbed mass under isothermal conditions	√	Large quantities
large temperature jump	Available both Gravimetric and volumetric versions	Pressure and temperature sensors (volumetric) Load cell (gravemtric)	Non-isothermal adsorption kinetics similar to real adsorption chiller operation	√	Small and Large quantities
Mass transfer from evaporator/condenser chamber to adsorber/desorber chamber	Mass flow integration	Micro-flow controller technique	Integration of mass flow through the mass controller	√	Large and small quantities

Table 5. Comparison of mathematical models

Model classification	Working Pair	Main features	Reference
Darcy model describes the flow in porous solid adsorbent and kinetics described by equilibrium Model	Methane/ activated carbon	▪ Low vapour flow velocity ▪ gas and solid are in thermodynamic equilibrium ▪ the equilibrium model was used to calculate the uptake where both the inter-particle mass transfer resistance(external resistance) and resistance inside particle (internal resistance) were neglected	Sahoo *et al.*[25]
Darcy model describes the flow in porous solid adsorbent and kinetics described by linear driving force , the diffusion resistance in the vapour phase was neglected (interparticle resistance neglected)	Ethanol/activated carbon	• low vapour flow velocity • inter-particle mass transfer resistance is neglected • The resistance in the adsorbent pore considered using LDF model where the average volume uptake is tracked with time and linear concentration gradient from particle center to surface is assumed. • LDF is a mathematically simplified version of solid diffusion model where the Fickian concentration derivative is replaced by linear difference in concentration(Parabolic concentration profile) • Validity of approach need to be checked to experimental data	Elsayed *et al.*[80]
Diffusion in porous solid considered while neglecting the inter-particle resistance in vapour	Ethanol/ Norit activated carbon RX3	• High capability of modelling the adsorption process in solid particle. • Constant pressure is assumed over the particle surface	Freni *et al.* [105], Elsayed *et al.* [107]
Both mass transfer resistances in porous solid and vapour domains were considered	Sws-1L/ water	• Diffusion processes were considered in both solid and vapour phases	Niazmand *et al.*[116]